(2)

ONR-URI Composites Program
Technical Report No. 24

UIUC-NCCMR-89-24

CREEP BUCKLING OF THERMOPLASTIC-MATRIX FIBER COMPOSITES UNDER BIAXIAL LOADING+

Y. Nakajo* and S.S. Wang**

December, 1989

National Center for Composite Material Research
at University of Illinois, Urbana - Champaign
A DoD University Research Initiatives Center funded by the
Office of Naval Research, Arlington, VA

+ in Journal of Thermoplastic Composite Materials, Vol. 2, No. 3, July 1989, pp. 172-215.

* Research Associate, NCCMR; Now Assistant Professor, Mechanical Engineering Department, Ashikaga Institute of Technology, Ashikaga City, Tochigi, 326, Japan.

** Professor of Theoretical and Applied Mechanics and of Aeronautical and Astronautical Engineering, and Director of National Center for Composite Materials Research.

ACKNOWLEDGMENT

This research was supported in part by the Office of Naval Research (ONR), Arlington, VA through Grants N00014-86-K-0799 and N00014-85-K-0654 and by du Pont Co., Wilmington, DE to the University of Illinos at Urbana-Champaign. The authors wish to express their gratitude to Drs. Rem Jones and Y. Rajapakse of ONR and Drs. J.K. Lees and K.B. Su of du Pont for their encouragement. Also, the technical assistance by Dr. A. Miyase of NCCMR during the course of the study is deeply acknowledged.

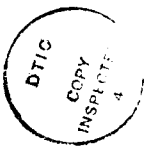

Elevated-Temperature Creep Buckling of Thermoplastic-Matrix Fiber Composites under Biaxial Loading

Y. NAKAJO* AND S. S. WANG**
Department of Mechanical and Industrial Engineering
University of Illinois
Urbana-Champaign, IL 61801

ABSTRACT: An analytical study has been conducted to investigate the elevated-temperature creep buckling behavior of thermoplastic-matrix composite laminates subjected to multiaxial loading. Anisotropic time-temperature dependent viscoelastic constitutive equations of the composite are constructed first, using the experimental results and the modified Prony series expansion solution. Creep buckling loads and associated creep failure times are determined by a time-dependent bifurcation buckling analysis of the thermoplastic composite laminates under general loading in an elevated-temperature environment. Detailed solutions for high-temperature creep buckling and associated failure mode shapes of the AS4/J1 thermoplastic composite laminates with various fiber orientations are obtained. The creep buckling mode shape changes and the accompanying failure loads are studied for three commonly encountered loading modes: (1) pure shear, (2) biaxial compression with any arbitrary stress biaxiality ratios, and (3) combined axial compression and shear loading.

1. INTRODUCTION

HIGH-TEMPERATURE THERMOPLASTIC-MATRIX COMPOSITES are currently considered to be used in high-performance structures such as supersonic aircraft. The advanced structural applications require accurate analyses and clear understanding of the failure behavior of structural elements at elevated temperatures. Among various structural failure problems presently concerned, elevated-temperature stability of thermoplastic-matrix composite panels under multiaxial loading is of significant interest not only because of its intrinsic complexities but also because of its technical importance.

Reprinted from *Proceedings of the Fourth Japan-U.S. Conference on Composite Materials, Washington, DC, June 27-29, 1988*, Lancaster, PA:Technomic Publishing Co., Inc. (1988).

* Post-doctoral Research Associate.
** Professor and Director.

0892-7057/89/03 0172-44 $4.50/0

The objectives of the present study are to introduce a proper mathematical method to account for high-temperature constitutive properties of the composites and to investigate fundamental creep buckling behavior of thermoplastic-matrix composite panels under general multiaxial loading in elevated-temperature environments.

The subject of creep buckling of structures has been studied by many researchers, and two common approaches have been taken. One is based on nonlinear power law creep stress-strain constitutive equation, representative of constitutive laws for most metal creep. Hoff [10] firstly proposes a rational criterion for this type of creep failure by introducing a critical time (i.e., buckling time) at which the initial imperfection grows to infinite amplitude. A brief history of this approach is introduced in Reference [11]. The other kind of creep buckling analysis is the one used for structures with hereditary-integral-type viscoelastic material constitutive equations. The definition of the critical time used in this approach with small deflection theory gives an infinite-long buckling time, which apparently contradicts to experimental results [12]. To alleviate this problem, for example, Hilton defines [7] the creep buckling time of a column as the one at which the deflection is of such a magnitude that the maximum moment in the column will reach the ultimate value the material can carry. Freudental [8] determines the critical time of a column by considering the divergence of successive approximations for the lateral deflection in terms of a power series, involving the applied load and time. The problem of creep buckling of a linear viscoelastic material has been investigated widely from the view point of growth of an initial imperfection [2,14,15,16]. Williams [4] and Powell [5] define the creep buckling time of a viscoelastic column based on a bifurcation buckling criterion. Recently, Wilson and Vinson [21] extend the viscoelastic linear buckling analysis to laminated composite columns using the correspondence principle to obtain the critical time. It is well-known that a direct application of the bifurcation-type analysis for creep buckling generally gives extremely modest estimation of the creep buckling time [10], as compared with Hoff's approach. However, each of the above analyses should give certain insights into the creep buckling failure behavior of high-temperature structures with different configurations.

In this research, a combined experimental and theoretical approach is taken to analyze the creep buckling problem of a thermoplastic-matrix composite panel at elevated temperatures. The experimental results obtained from accompanying studies [17,20,22] are used for material considerations. A recently developed method with the aid of an optimization theory is introduced first to describe the long-term anisotropic viscoelastic behavior of the composite. Accuracy and convergence of the solutions are studied in detail. The well-known transform method is then used to study the creep instability of the thermoplastic-matrix composite panels with several different fiber orientations. Three loading modes are considered in the study: (1) pure shear, (2) biaxial compression of arbitrary biaxial stress ratios, and (3) combined axial compression and shear loading. The results obtained in this study provide important information to our understanding of the elevated-temperature instability of the thermoplastic-matrix composite panel under general loading modes.

2. METHODS OF APPROACH

2.1 Anisotropic Viscoelastic Constitutive Equations for Unidirectional Composites

In the development of analytical methods to study elevated-temperature creep buckling behavior of a thermoplastic-matrix composite, time-temperature-dependent constitutive equations of the composite must be determined first. In this study, the anisotropic viscoelastic creep compliance data of a unidirectional thermoplastic fiber composite obtained in the related studies [17,20,22] are used for construction of material constitutive equations. The master curves of creep compliances of the composite are determined by applying the time-temperature equivalence principle. The transverse compliance J_{22} and the shear compliance J_{66} of the composite are directly measured in the elevated-temperature creep experiments. The time-temperature-dependent Poisson's ratio ν_{12} is determined by the use of the rule of mixtures [1], based on the properties of neat matrix resin and the fibers at different temperatures and by properly shifting the data to construct the master curve. The longitudinal modulus is assumed to be temperature- and time-independent.

The composite viscoelastic constitutive equations are expressed in the following forms of Equations (2-1-1) and (2-1-2), for the thermoplastic matrix composite.

$$J_{ij}(T,t) = C_{ij}^{(0)}(T) + \sum_{k=1}^{n} C_{ij}^{(k)}(T) \exp\left[\mu_k(T)t\right] \tag{2-1-1}$$

$$\nu_{ij}(T,t) = D_{ij}^{(0)}(T) + \sum_{k=1}^{n} D_{ij}^{(k)}(T) \exp\left[\gamma_k(T)t\right] \tag{2-1-2}$$

where $C_{ij}^{(k)}$, $D_{ij}^{(k)}$, μ_k and γ_k are coefficients dependent on the temperature and fiber orientations.

To express the experimental data of the anisotropic composite properties by proper analytical expressions, a sequential unconstrained minimization technique (SUMT) is used in this study. Details of the SUMT is given in Appendix 1. Curve fitting for a longer time range requires the introduction of several new features in the solution procedure, including (1) use of sufficient number of terms, (2) introduction of additional constraint conditions, and (3) selection of proper initial values. The use of sufficient terms in Equation (2-1-1) is most essential because the time range which one term can cover is limited only to a few decades at most, and the regions near to both ends of the time range of interest need sufficient terms. An accurate solution in the desired time range requires many terms but, on the contrary, most of the terms are used to fit the end portions of the curve (see Appendix 1). And very often the resolutions are lost because of the limit of the precision in the calculation.

Besides the original constraint for $\mu_k(t)$ due to physical feasibility, additional constraint conditions are introduced not only to accelerate the convergence but also to prevent the solution from having the oscillating feature, which sometimes introduces a small error. Besides these additional conditions, the use of many terms itself increases the number of constraint conditions.

With increase in number of terms, proper selection of initial values becomes difficult. The SUMT method is employed to solve the problem efficiently with above three requirements. The procedure has demonstrated to minimize the discrepancies between experimental data and modified Prony series solution under these constraint conditions.

2.2 Viscoelastic Composite Laminate Theory

Owing to the elevated temperature environment considered, viscoelastic composite laminate theory needs to be used to analyze the creep buckling behavior of thermoplastic-matrix composites with various ply orientations. Specifically, the classical lamination theory is modified to include the viscoelastic composite constitutive equations. The use of the well-known correspondence principle [4] facilitates the analytical procedure of the composite creep buckling analysis. In the present study, only symmetric angle-ply composite laminates are considered. As a result, in-plane and out-of-plane displacements are decoupled in the viscoelastic composite plate equations [3].

Based on the correspondence principle, the elastic composite laminate theory forms the basis of the viscoelastic composite analysis. Consequently one obtains the corresponding elastic governing equation for the deflection of the composite plate:

$$D_{xx}\frac{\partial^4 w}{\partial x^4} + 4D_{xs}\frac{\partial^4 w}{\partial x^3 \partial y} + 2(D_{xy} + 2D_{ss})\frac{\partial^4 w}{\partial x^2 \partial y^2} + 4D_{ys}\frac{\partial^4 w}{\partial x \partial y^3} + D_{yy}\frac{\partial^4 w}{\partial y^4} + N_x\frac{\partial^2 w}{\partial x^2} + N_y\frac{\partial^2 w}{\partial y^2} - 2N_{xy}\frac{\partial^2 w}{\partial x \partial y} = 0 \tag{2-2-1}$$

where

$$D_{\alpha\beta} = 2\sum_{k=1}^{n}\int_{h_{k-1}}^{h_k} z^2 E_{\alpha\beta}^{(k)} dz \qquad (\alpha,\beta = x,y,s) \tag{2-2-2}$$

$$E_{xx} = \frac{E_{22}\cos^4\theta}{1 - \nu_{12}\nu_{21}} + 2\left(\frac{\nu_{12}E_{22}}{1 - \nu_{12}\nu_{21}} + 2G_{66}\right)\sin^2\theta\cos^2\theta + \frac{E_{11}\sin^4\theta}{1 - \nu_{12}\nu_{21}}$$

$$E_{yy} = \frac{E_{22}\cos^4\theta}{1 - \nu_{12}\nu_{21}} + 2\left(\frac{\nu_{12}E_{22}}{1 - \nu_{12}\nu_{21}} + 2G_{66}\right)\cos^2\theta\sin\theta^2 + \frac{E_{11}\sin^4\theta}{1 - \nu_{12}\nu_{21}} \tag{2-2-3}$$

in which θ is the off axis angle, and the numeric subscripts of the material properties denote those in material coordinates (Figure 2-2-1).

The solution for the above governing differential equation along with proper B.C.'s of a given composite panel can be determined by various methods. The viscoelastic solution can then be derived, using the correspondence principle later.

2.3 Viscoelastic Creep Buckling Analysis of Thermoplastic-Matrix Composite Laminates

In this study, Galerkin's method [3] is used to obtain the corresponding elastic buckling solution. The elastic solution is then converted into viscoelastic solutions by the correspondence principle which is technically the inverse Laplace transformation of the elastic solution after replacing the compliances J_{ij} with sJ_{ij} and the Poisson's ratio ν_{ij} with $s\nu_{ij}$. By replacing the associated material properties, the elastic solution becomes identical to the viscoelastic solution in the Laplace domain, or s-domain. Hence, inverse Laplace transformation of the elastic solution with the replaced material properties gives the viscoelastic solution in the real time domain. The critical time of structural instability for a thermoplastic composite laminate with the viscoelastic properties is subsequently calculated from the solution obtained by above referenced technique based on a bifurcation buckling analyses of a composite laminate.

2.3.a THE GALERKIN'S METHOD

The lateral deflection w_{as} for a simply-supported retangular composite plate is assumed as

$$w_{as} = \sum_{m=1}^{2} \sum_{n=1}^{2} c_{mn} \sin \frac{m\pi x}{L_x} \sin \frac{n\pi y}{L_y} \tag{2-3-1}$$

According to the well-known Galerkin's method, the following equations can be obtained:

$$\begin{vmatrix} \dfrac{\pi^2 L_x L_y}{4}\left(\pi^2 F_{11} - \dfrac{N_x}{L_x^2} - \dfrac{N_y}{L_y^2}\right) - \dfrac{32}{9}(8\pi^2 S_{11} + N_{xy}) & \\ -\dfrac{32}{9}(2\pi^2 S_{11} + N_{xy}) & \pi^2 L_x L_y\left(4\pi^2 F_{11} - \dfrac{N_x}{L_x^2} - \dfrac{N_y}{L_y^2}\right) \end{vmatrix} = 0 \tag{2-3-2a}$$

$$\begin{vmatrix} \dfrac{\pi^2 L_x L_y}{4}\left(\pi^2 F_{12} - \dfrac{N_x}{L_x^2} - \dfrac{4N_y}{L_y^2}\right) - \dfrac{32}{9}(2\pi^2 S_{21} + N_{xy}) & \\ -\dfrac{32}{9}(2\pi^2 S_{12} + N_{xy}) & \dfrac{\pi^2 L_x L_y}{4}\left(\pi^2 F_{21} - \dfrac{4N_x}{L_x^2} - \dfrac{N_y}{L_y^2}\right) \end{vmatrix} = 0 \tag{2-3-2b}$$

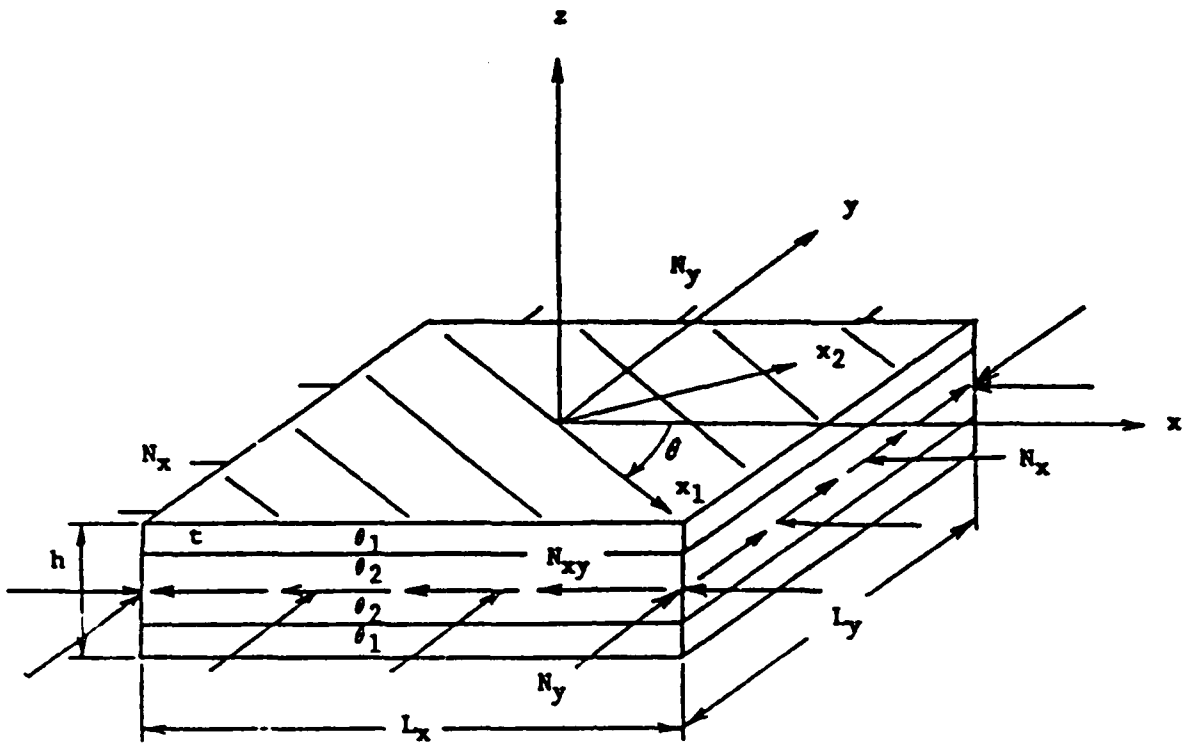

Figure 2-2-1. *Asymmetric composite laminates with $[\theta_1/\theta_2/\theta_2/\theta_1]$ fiber orientations under general inplane compression and shear loading.*

where

$$S_{ij} = (i/L_x)^2 D_{xs} + (j/L_y)^2 D_{ys}$$
$$F_{ij} = (i/L_x)^4 D_{xx} + 2(i/L_x)^2 (j/L_y)^2 (D_{xy} + 2D_{ss}) + (j/L_y)^4 D_{yy}$$

To solve for N_x, N_y, and N_{xy}, each equation has to contain only one unknown. For the pure shear case, the unknown is N_{xy} and $N_x = N_y = 0$. For the case of combined axial compression and shear or the biaxial compression, either one of the two loads must be the unknown and the other must have a known value. In this study, N_x is chosen to be the unknown for the latter two cases, and the constant values of other loads, i.e., N_y for the biaxial compression and N_{xy} for the combined axial compression and shear, are changed parametrically. By using the Galerkin's method, the governing differential equation is discretized into simultaneous equations. For the assumed deflection Equation (2-3-1), the set of simultaneous equations is further divided into two sets of simultaneous equations (see Appendix 5). The solution obtained from Equation (2-3-2a) has contribution of two components in the assumed deflection which are expressed by $m = 1$, $n = 1$ and $m = 2$, $n = 2$ in Equation (2-3-1) shown in Figure 2-3-1. And the solution from Equation (2-3-2b) has the ones which correspond to $m = 1$, $n = 2$ and $m = 2$, $n = 1$. No other mode coupling exists except for those combinations. The lowest load should be chosen among the four roots for each buckling load obtained from Equations (2-3-2a) and (2-3-2b).

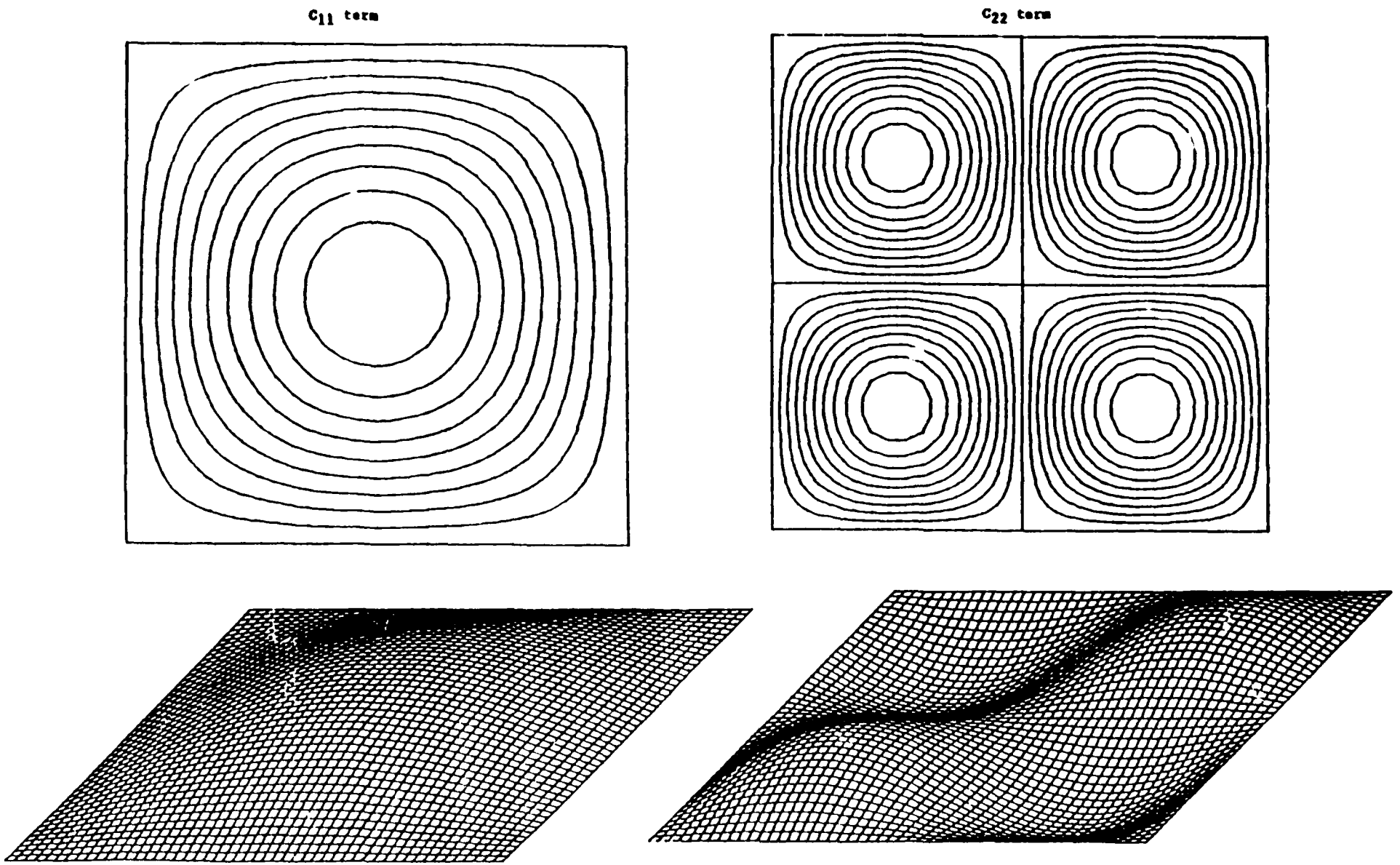

Figure 2-3-1. *Buckling shape corresponding to each term in Equation (2-3-1).*

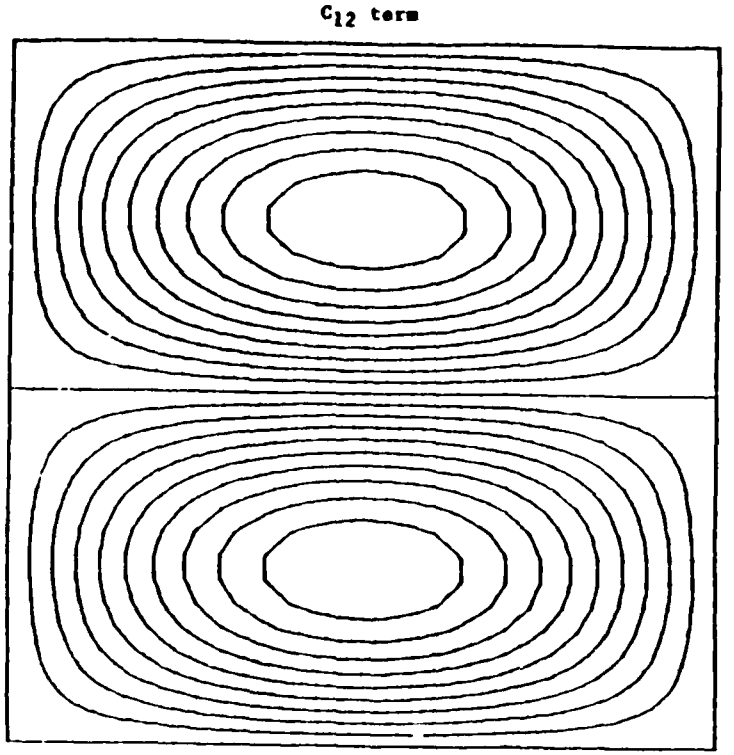

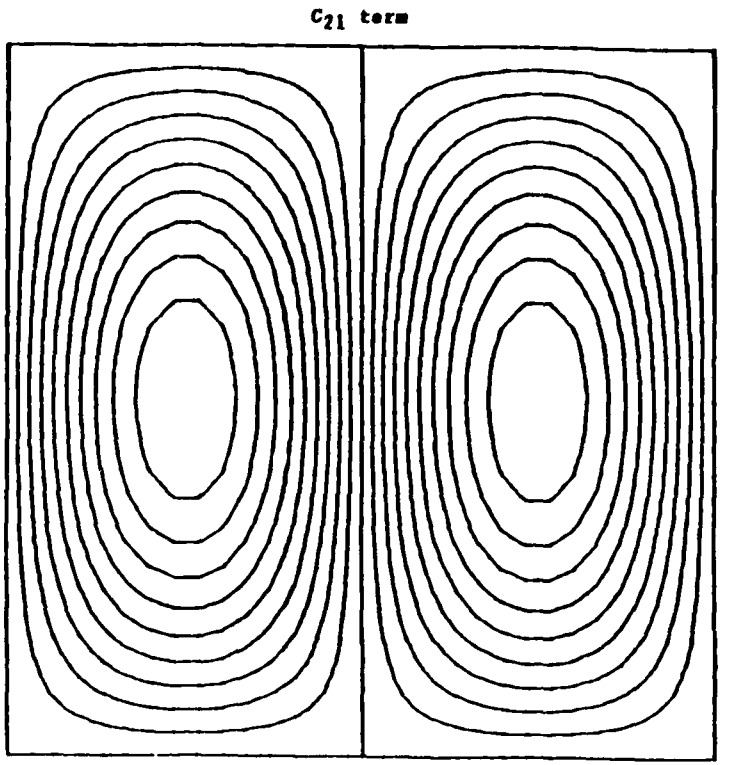

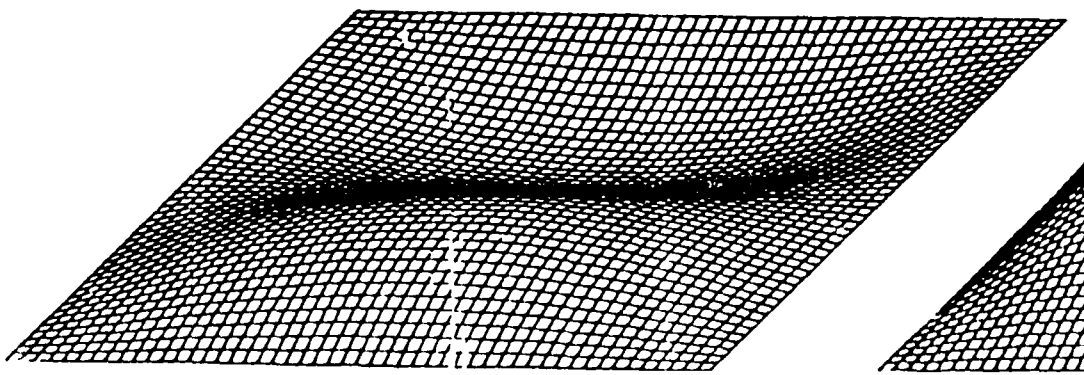

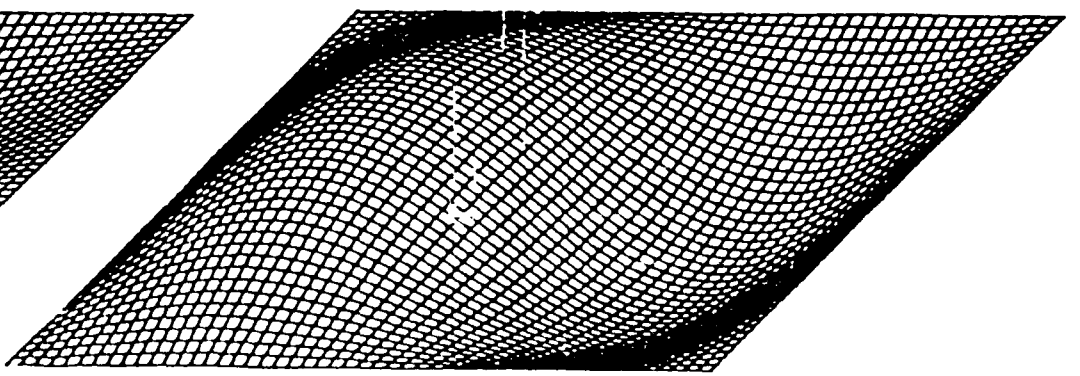

Figure 2-3-1 (continued). *Buckling shape corresponding to each term in Equation (2-3-1).*

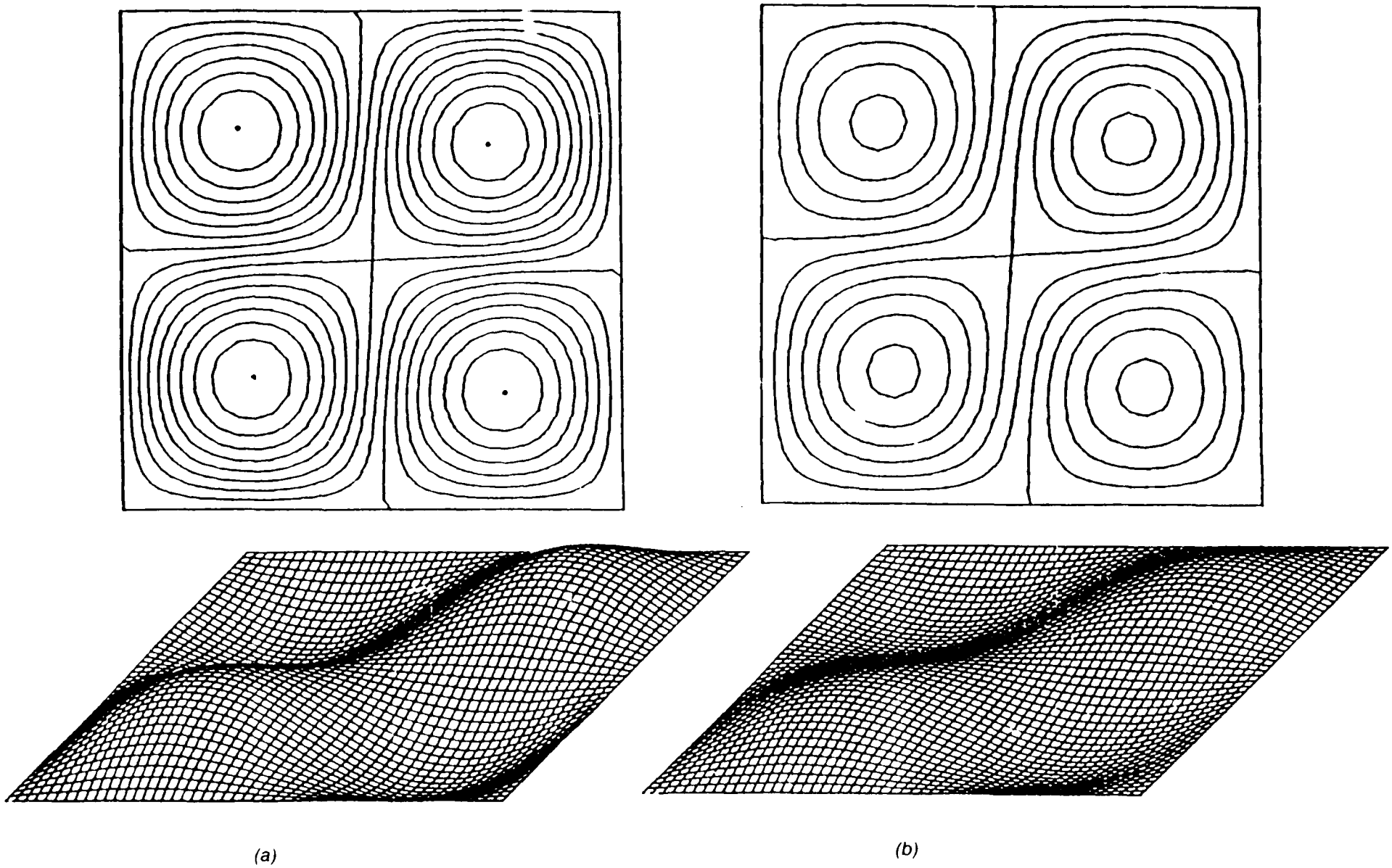

(a) (b)

Figure 2-3-2. *Elastic buckling mode shape: (a) pure shear loading; (b) combined axial compression and shear ($\tau_{12}^{*} = 0.5\tau_{12}^{*}$).*

2.3.b INVERSE LAPLACE TRANSFORMATION FOR VISCOELASTIC CREEP BUCKLING

Once the elastic solution is obtained, the use of the correspondence principle leads to the viscoelastic solution. For example, expanded explicit form of Equation (2-3-2b) for angle-ply laminates in VE domain are:

$$\pi^4\left(\frac{2}{3}t^3\right)^2\left[\frac{16}{L_x^8}B_1+\frac{136}{L_x^6L_y^2}B_2+\frac{272}{L_x^6L_y^2}B_3+\frac{257}{L_x^4L_y^4}B_4+\frac{64}{L_x^4L_y^4}B_5\right.$$

$$\left.+\frac{256}{L_x^4L_y^4}B_6+\frac{256}{L_x^4L_y^4}B_7+\frac{136}{L_x^2L_y^6}B_8+\frac{272}{L_x^2L_y^6}B_9+\frac{16}{L_y^8}B_{10}\right]$$

$$-\pi^2\frac{2t^3}{3}\left(\frac{4N_x}{L_x^2}+\frac{N_y}{L_y^2}\right)B_{11}-\pi^2\frac{2t^3}{3}\left(\frac{N_x}{L_x^2}+\frac{4N_y}{L_y^2}\right)B_{12}$$

$$+\left(\frac{4N_x}{L_x^2}+\frac{N_y}{L_y^2}\right)\left(\frac{N_x}{L_x^2}+\frac{4N_y}{L_y^2}\right)B_{13}$$

$$-\left(\frac{128}{9\pi^2L_xL_y}\right)^2\left[4\pi^4\left(\frac{2}{3}h^3\right)^2(-1+2c^3)^2\left\{\frac{4}{L_x^4}B_{14}+\frac{4}{L_y^4}B_{15}+\frac{17}{L_x^2L_y^2}B_{16}\right\}\right.$$

$$\left.+2\pi^2\frac{-t^2}{2}(B_{17}+B_{18})N_{xy}+N_{xy}^2B_{13}\right]=0 \qquad (2\text{-}3\text{-}4)$$

where B_1 to B_{18} are time-dependent coefficients. The B_1 for example has the form:

$$\begin{aligned}B_1 &= \sin^8\theta I_{0002}+4\sin^4\theta\cos^4\theta[E_{11}^2I_{0222}+4E_{11}(I_{0121}I_{1221})\\&\quad+4(I_{0020}-2I_{1120}+I_{2220})]+E_{11}^2\cos^8\theta I_{0022}\\&\quad+4\cos^2\theta\sin^6\theta[E_{11}I_{0112}+2I_{0011}-2I_{1111}]\\&\quad+4E_{11}\cos^6\theta\sin^2\theta[E_{11}I_{0122}+2I_{0021}-2I_{1121}]\\&\quad+2E_{11}\cos^4\theta\sin^4\theta I_{0012} \qquad (2\text{-}3\text{-}5)\end{aligned}$$

in which

$$I_{ijkl}=\pounds^{-1}\left\{\frac{1}{s^{8-(i+j+k+1)}}\nu_{12}^{(i)}\nu_{21}^{(j)}J_{22}^{(k)}J_{66}^{(l)}\right\} \qquad (2\text{-}3\text{-}6)$$

Solutions for general angle-ply laminates including the degenerated cases of a unidirectional composite by letting $\theta = 0$ and a cross-ply laminate are shown in

the Appendices 2, 3 and 4. The inverse Laplace transformation, Equation (2-3-6), can be calculated by the use of convolution integral. For example, the I_{2222} term has the form

$$I_{2222} = \int_0^t \int_0^\tau \int_0^p \nu_{12}(u)\nu_{12}(p-u)du \int_0^{\tau-p} \nu_{21}(v)\nu_{21}(\tau-p-v)dvdp$$
$$\times \int_0^{t-\tau} \int_0^q J_{22}(\xi)J_{22}(q-\xi)d\xi \int_0^{t-\tau-q} J_{66}(\eta)J_{66}(t-\tau-q-\eta)d\eta dqd\tau \tag{2-3-7}$$

The mode shape change is also calculated by making use of the correspondence principle. The ratios c_{11}/c_{22} and c_{12}/c_{21} can be conveniently used to represent the buckling modes. For example, c_{11}/c_{22} for the angle-ply laminate is calculated from the simultaneous equations (see Appendix 5) from which Equation (2-3-2a) is obtained with a condition for nontrivial solution for c_{11} and c_{22} as

$$\frac{c_{11}}{c_{22}} = \frac{32}{9}\frac{4}{\pi^2 L_x L_y}\frac{8\pi^2 S_{11} + N_{xy}}{\pi^2 F_{11} - (N_x/L_x^2) - (N_y/L_y^2)} \tag{2-3-8}$$

Hence

$$c_{11}\left[\pi^2\left\{\frac{D_x}{L_x^4} + 2(D_{xy} + 2D_s)\frac{1}{L_x^2 L_y^2} + \frac{D_y}{L_y^4}\right\} - \frac{N_x}{L_x^2} - \frac{N_y}{L_y^2}\right.$$
$$\left. - c_{22}\frac{128}{9\pi^2 L_x L_y}\left\{8\pi^2\left(\frac{D_{xs}}{L_x^2} + \frac{D_{ys}}{L_y^2}\right) + N_{xy}\right\} = 0\right. \tag{2-3-9}$$

Applying the correspondence principle, the above equation is transformed into the real time domain as:

$$c_{11}\left[\pi^2\left\{\frac{2}{3}h^2\left(A_5 I_{0012} + A_6 I_{0022} + A_7 I_{0122} + A_8(I_{0021} - I_{1121})\right)\right\}\right.$$
$$\left. - \left(\frac{N_x}{a^2} + \frac{N_y}{b^2}\right)(I_{0022} - I_{1122})\right] - c_{22}\frac{128}{9\pi^2 L_x L_y}\left[8\pi^2\left\{\frac{2}{3}h^2(-1 + 2c^3)\right.\right.$$
$$\left.\left.(A_1 I_{0012} - A_2 I_{0022} + A_3 I_{0122} + A_4(I_{0021} - I_{1121}))\right\} + N_{xy}(I_{0022} - I_{1122})\right] = 0 \tag{2-3-10}$$

where A_1 to A_8 are constants (see Appendix 2). The equations to be solved for other modes are shown in Appendix 5. The ratio of the amplitude c_{11}/c_{22} can be

calculated for the applied load by substituting the buckling time (for example 100 minutes in the present analysis) to determine the parameters I_{ijkl}.

3. RESULTS AND DISCUSSION

To illustrate the fundamental behavior of elevated-temperature creep buckling of thermoplastic-matrix fiber composites, analytical solutions have been obtained for a carbon fiber (AS4) reinforced polyamide (J1) matrix composite under various in-plane, biaxial compression and/or shear loading. The AS4/J1 thermoplastic matrix composite considered here has a glass-transition temperature $T_g \cong 293°F$ (145°C). Anisotropic viscoelastic constitutive properties are determined by the use of the elevated-temperature experimental data. The elastic modulus along fiber direction, E_{11}, is assumed to be time- and temperature-independent with the value of 1.75×10^7 psi. Creep buckling behavior of the unidirectional AS4/J1 composite is studied first to provide a general reference for the subsequent analysis of more complex, multilayered angle-ply and cross-ply thermoplastic composite laminates.

For both cases of the unidirectional composite and multilayered laminates the panels have dimensions, $L_x = 10$ inch, and $L_y = 10$ inch, and a uniform ply thickness $h = 0.2$ inch (Figure 2-2-1). Three multiaxial loading modes are considered: (a) pure shear loading, (b) combined axial compression and shear, and (c) biaxial compression with arbitrary stress biaxiality ratios. For each case, a schematic is shown in the respective figure. The nominal shear stress and the nominal compressive stress in the y direction are changed parametrically in the analyses for the cases (b) and (c), respectively. In all of the cases studied, creep buckling loads, critical instability times, and associated buckling mode shapes of the composite laminates under various combinations of in-plane biaxial compression and shear are determined for several temperatures. The degenerated solution, i.e., the thermoelastic buckling solution, for each case is also determined and included here for the reference purpose.

3.1 Analytical Expression of Anisotropic Viscoelastic Composite Constitutive Equations

In the use of the correspondence principle for studying the thermoplastic composite constitutive equations, only the time dependency is taken into account. The temperature effect can be introduced into the analyses by the time-temperature equivalence concept [19]. Owing to the fact that the time dependency of the composite results mainly from the matrix [22], the time-temperature equivalence is isotropic. Therefore the shift factor of the matrix can be used to relate any of the solutions obtained in the present analysis at 145°C to that at a desired temperature. While any solution at a given temperature can be shifted to that at a different temperature, the expressions of the viscoelastic material properties in the present analysis is valid only for the time range of five decades.

The numbers of terms used in the modified Prony series expansion of J_{22}, J_{66} and ν_{12} are determined for the solutions within an admissible range of approximation. The present method can theoretically give precise fitting for a long

range by using increased number of terms. However, owing to the resolution of numerical results, the use of many terms (e.g., $n > 15$) may now work out for too long a time range. At present, the upper limit of the time range is 5 decades in a a log scale, which can be shifted to another portion of the master curve. But it is very difficult to expand to the range of more than 5 decades. Figure 3-1-5 shows the difficulties to extend the ends by adding additional terms. Sometimes close values of the design variables β_i's lead to the same local optimum value (see Table 3-1-1). The more this happens, the greater the advantage of starting the optimization using many terms is lost. In the present analyses initial values are determined by the next equation.

For β_i's,

$$\beta_i = 1 - g^i - h \qquad (i = 1,n) \tag{3-1-1}$$

where $0 < g < 1$, $h \ll 1$. For C_i's (after normalization),

$$C_0 = 1.2$$

$$C_i = -0.01 \qquad (i = 1,n) \tag{3-1-2}$$

The order in Tables 3-1-1 to 3-1-3 corresponds to the order of the initial values in Equation (3-1-1).

Convergence of the series solution with different numbers of terms can be seen from Figure 3-1-5 which shows the feature of each normalized term for representative β_i values in Equation (2-1-1). To extend the range to the direction of $t = 0$,

Table 3-1-1. Various terms in modified Prony series for composite creep compliance J_{22} at T = 293°F (145°C).

k	$C_{22}^{(k)}$ (psi^{-1})	μ_k
1	-1.452100E-07	-2.514420E+00
2	-1.146764E-07	-1.277711E+00
3	-9.236675E-08	-7.365715E-01
4	-6.734417E-08	-3.161159E-01
5	-5.990098E-08	-1.569684E-01
6	-6.721540E-08	-8.364243E-02
7	-8.490632E-08	-4.535500E-02
8	-1.027089E-07	-2.200023E-02
9	-1.134783E-07	-7.457791E-03
10	-1.189835E-07	-6.627651E-04
11	-1.202688E-07	-1.065326E-03
12	-1.221522E-07	-1.602799E-04
13	-1.227818E-07	-2.869180E-05
14	-1.227750E-07	-2.869180E-05
15	-1.228800E-07	-2.869180E-05

Table 3-1-2. Various terms in modified Prony series for composite creep compliance J_{66} at T = 293°F (145°C).

k	$C_{66}^{(k)}$ (psi^{-1})	μ_k
1	−2.003911E−07	−2.501196E+00
2	−1.658524E−07	−1.275838E+00
3	−1.454192E−07	−7.355021E−01
4	−1.342051E−07	−3.151077E−01
5	−1.507481E−07	−1.553528E−01
6	−1.900140E−07	−8.061813E−02
7	−2.433190E−07	−3.992683E−02
8	−2.891804E−07	−1.451749E−02
9	−3.089745E−07	−3.267287E−03
10	−3.123734E−07	−1.370418E−03
11	−3.129629E−07	−5.621973E−05
12	−3.128881E−07	−5.621973E−05
13	−3.126838E−07	−5.621973E−05
14	−3.124806E−07	−7.796962E−04
15	−3.124339E−07	−1.155590E−03

Table 3-1-3. Various terms in modified Prony series for Poisson's ratio ν_{12} at T = 293°F (145°C).

k	$D^{(k)}$	γ_k
1	−1.015074E−02	−2.497946E+00
2	−6.755615E−03	−1.274916E+00
3	−5.396313E−03	−7.349936E−01
4	−3.690511E−03	−3.148159E−01
5	−2.069948E−03	−1.554924E−01
6	−1.485730E−03	−8.283169E−02
7	−4.751751E−03	−4.716623E−02
8	−8.328338E−03	−2.804054E−02
9	−1.099923E−02	−1.586411E−02
10	−1.283541E−02	−5.166782E−03
11	−1.510358E−02	−4.046428E−05
12	−1.597748E−02	−3.410993E−04
13	−1.621792E−02	−4.046428E−05

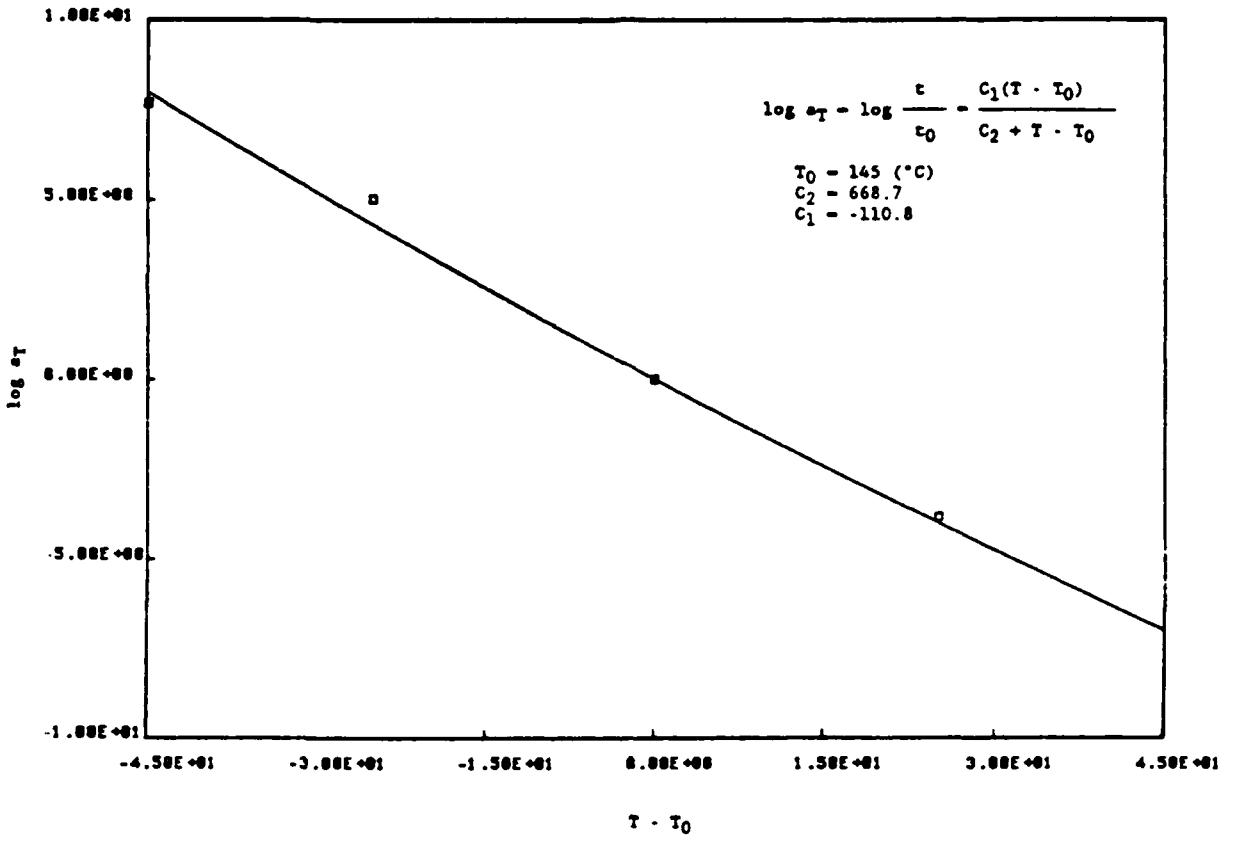

Figure 3-1-1. Shift factor vs temperature for AS4/ J1 thermoplastic-matrix composite [reference temperature = 293°F (145°C)].

the use of many terms with very small β_i values is necessary. To extend the range to the direction of $t = \infty$, additional terms with very close β_i values are necessary. In both cases, the resolution is easily lost by numerical errors during calculations. Also in this figure, it is apparent that a few terms used can cover only 2 or 3 decades over a log time scale at most, which is independent of the scheme of optimization or accuracy of calculation.

Figure 3-1-1 shows the relation between the temperature and the shift factor by

$$\log a_T = \frac{C_1(T - T_0)}{C_2 + T - T_0} \tag{3-1-3}$$

which is sometimes referred to as the WFL equation [19]. Values of the C_1 and C_2 are experimentally determined constants, T is a temperature and T_0 is a reference temperature. Conventionally C_1 and C_2 are obtainable by a graphical method as a gradient and an intercept in the $(T - T_0)/\log a_T$ vs. $T - T_0$ curve. In the present data reduction, a least-square method is employed to obtain C_1 and C_2. When a glass transition temperature T_g is used for T_0, it is known that C_1 and C_2 give approximately consistent values regardless of the material for the temperature range $T = T_g - 50°C$ to $T = T_g + 50°C$. The C_1 and C_2 values obtained from our experimental results differ from those consistent values [19].

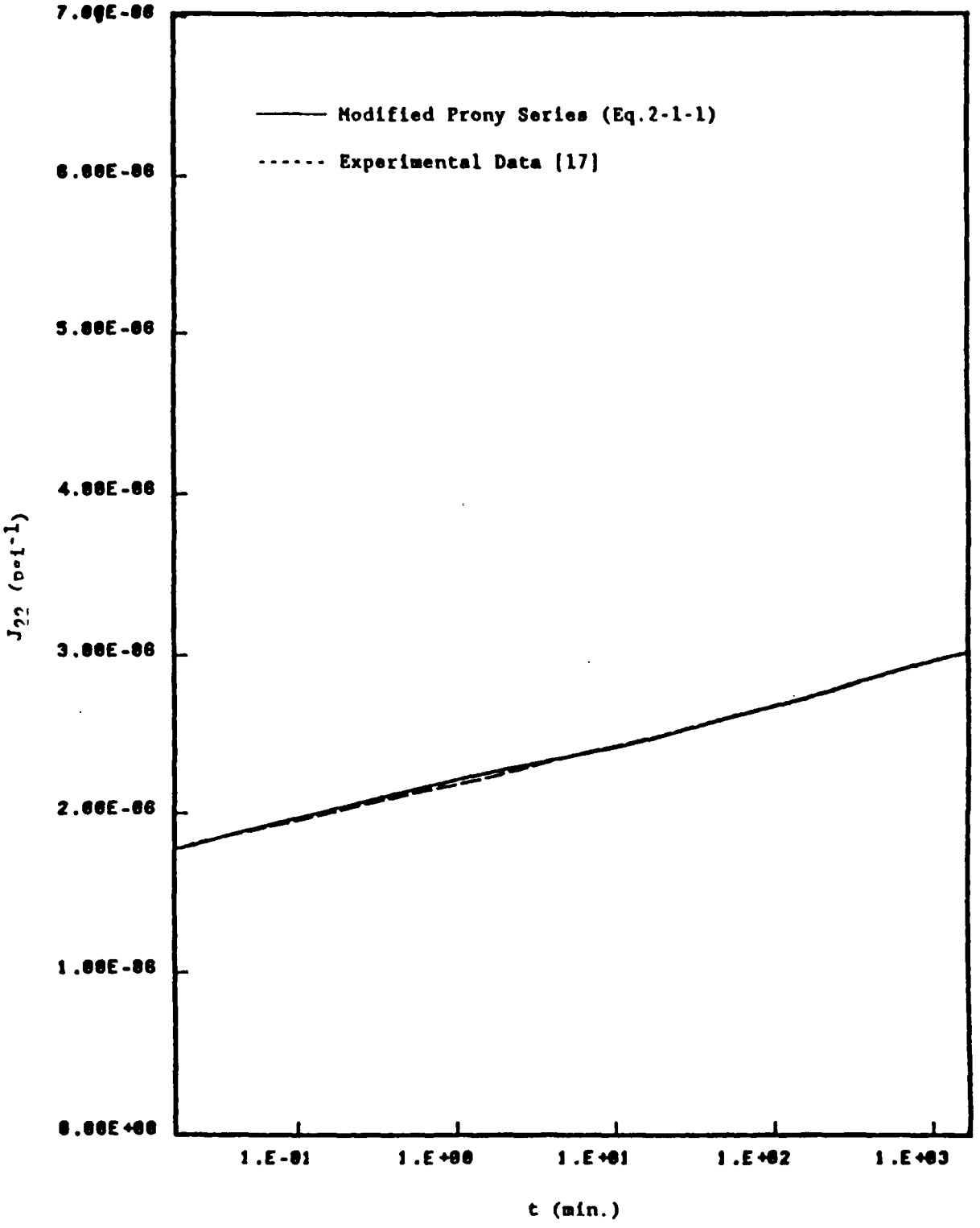

Figure 3-1-2. *High-temperature creep experimental data and the modified Prony series solution for AS4/J1 thermoplastic composite at T = 293°F (145°C).*

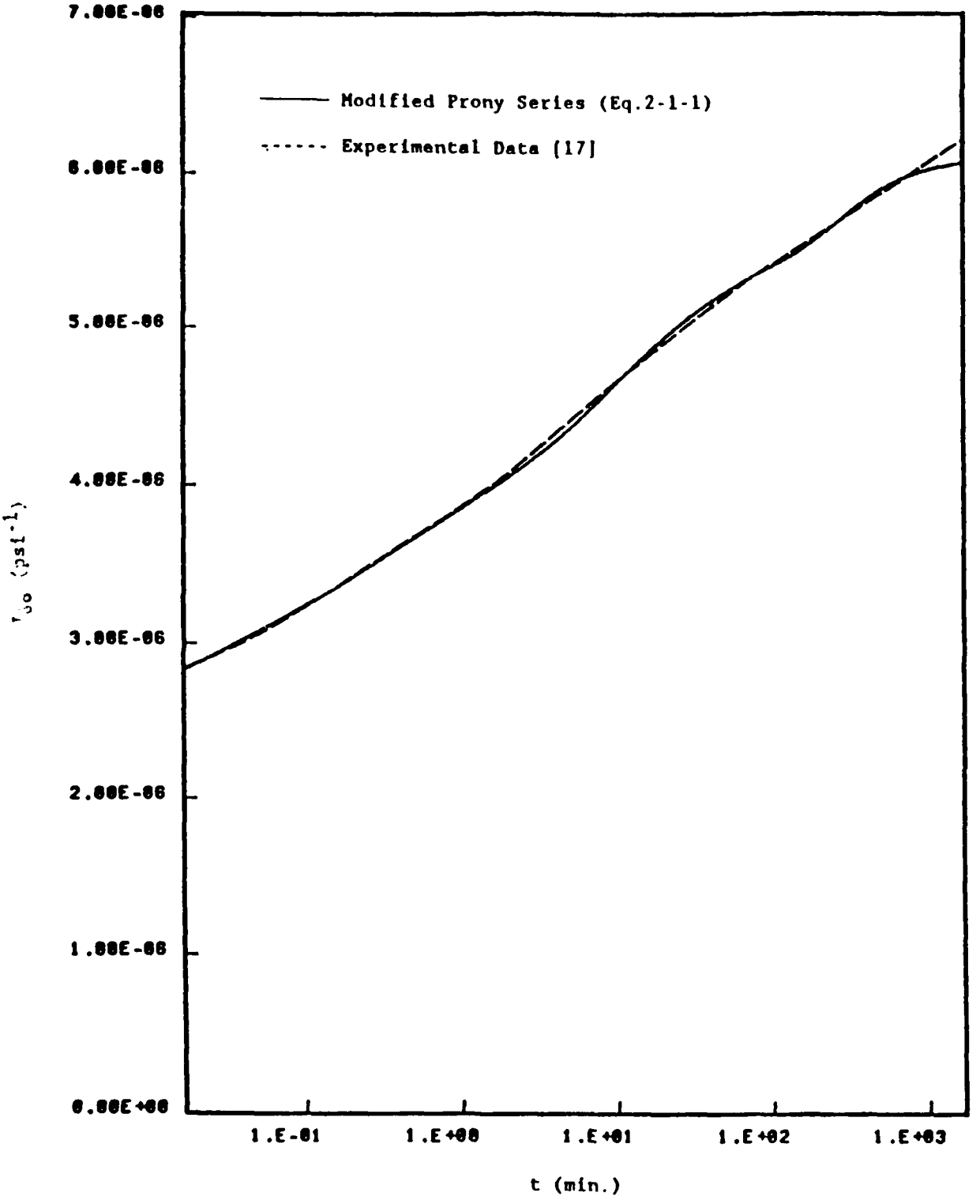

Figure 3-1-3. *High-temperature creep experimental data and the modified Prony series solution for AS4/J1 thermoplastic composite at T = 293°F (145°C).*

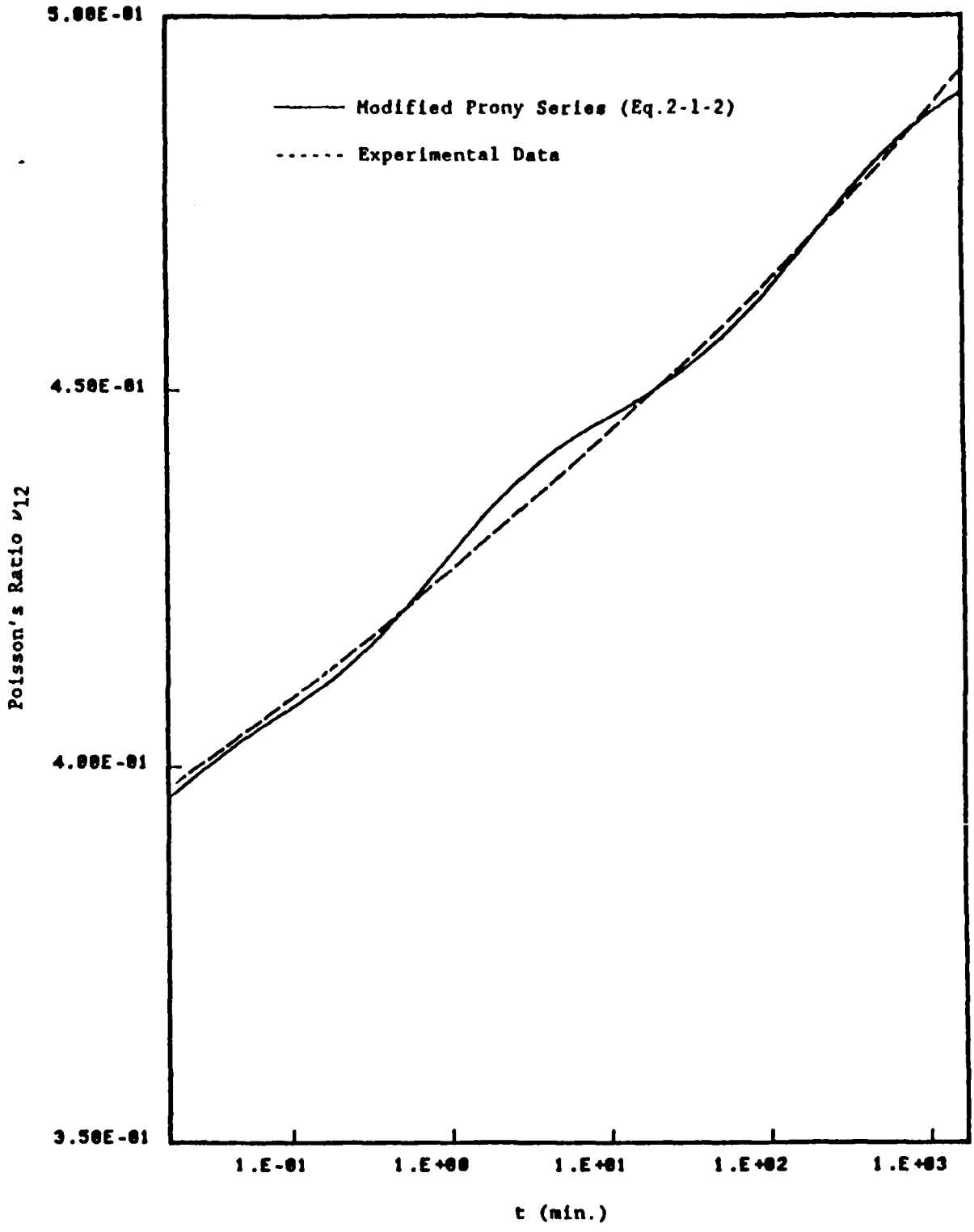

Figure 3-1-4. *High temperature creep experimental data and the modified Prony series solution for AS4/J1 thermoplastic composite at T = 293°F (145°C).*

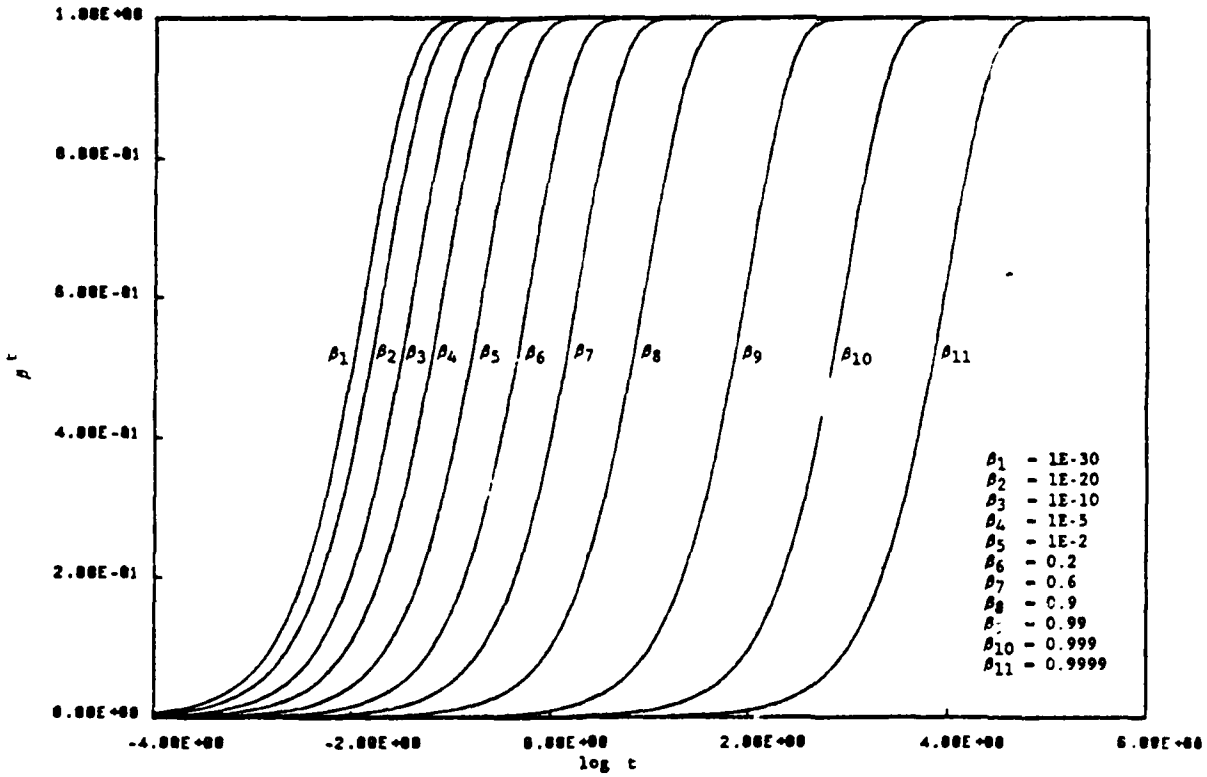

Figure 3-1-5. *Each normalized term for representative β_i values in Equation (2-1-1).*

3.2 Creep Buckling of Unidirectional Thermoplastic-Matrix Composites

3.2.a PURE SHEAR LOADING

As a reference for studying the elevated-temperature creep buckling of more complex composite laminates, thermal elastic buckling of a unidirectional composite panel, i.e., $\tau_{12}^{*} = \tau_{12}^{\infty}(0, T_g)$ is introduced first. The τ_{12}^{*} in Figure 3-2-1 is the elastic bifurcation buckling load calculated with the composite thermoelastic properties at the glass transition temperature $T = 145°C$. The value of τ_{12}^{*} is 19.36 ksi. The relationship between creep stress and creep buckling failure time of the composite at various temperatures is shown in the figure. The shift factor a_T is used for calculating buckling failure at various T's. The results at the glass transition temperature T_g ($= 293°F$) are also presented for comparison purposes. Above the glass transition temperature, the creep buckling failure becomes apparently more sensitive to the applied load. In other words, a small change in the applied load leads to a large change in the creep buckling time at $T > T_g$. In the case of an elastic bifurcation buckling, the critical load can be uniquely determined for a given composite structure. However, in the present creep buckling studies, creep buckling loads depend upon the time-dependent material properties. For more complex loading modes, the creep buckling results are shown in Figures 3-2-1 to 3-2-7 for both unidirectional and multilayered angle-ply and cross-ply thermoplastic composite laminates.

3.2.b BIAXIAL COMPRESSION

In Figure 3-2-2 the relationship between the biaxial creep stresses $\sigma_1^{\infty}(t,T)$ and $\sigma_2^{\infty}(t,T)$ and the associated creep failure times t is shown. [The buckling

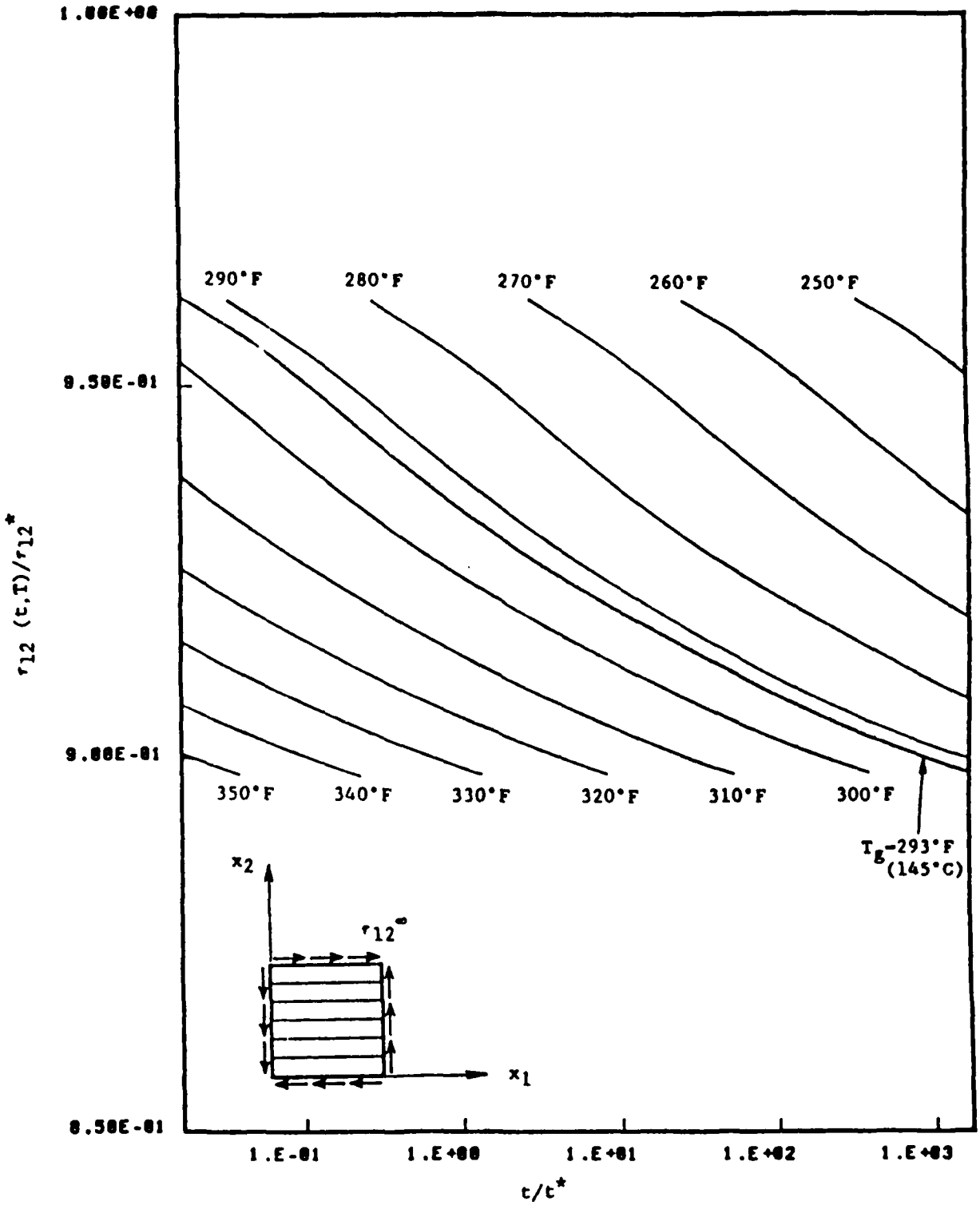

Figure 3-2-1. *Creep buckling failure of AS4/ J1 thermoplastic-matrix composite panel under pure shear loading at various temperatures (t^* = 1 min.).*

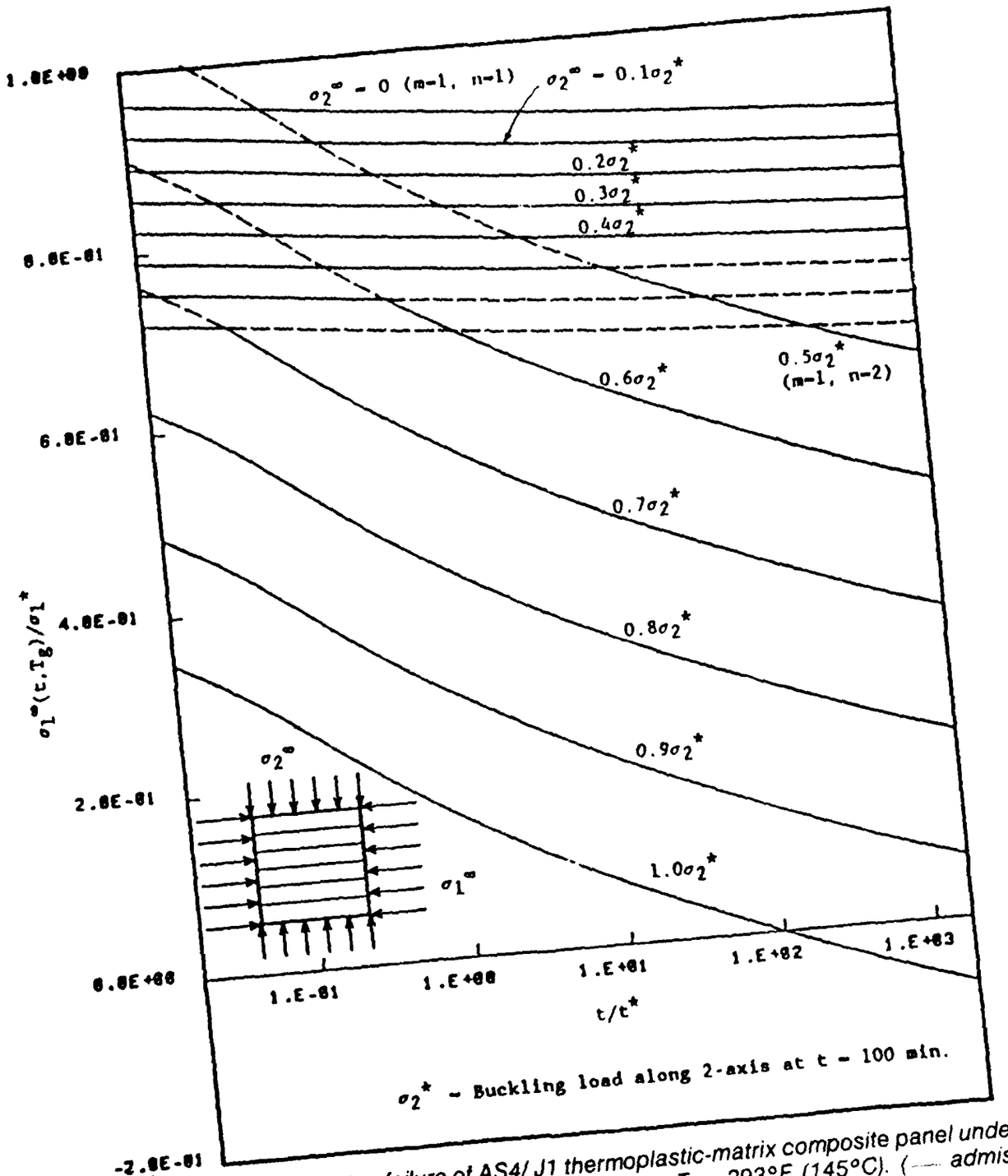

Figure 3-2-2. *Creep buckling failure of AS4/ J1 thermoplastic-matrix composite panel under biaxial compression of various stress biaxiality ratios at T = 293°F (145°C). (—— admissible solution, ---- unadmissible solution.)*

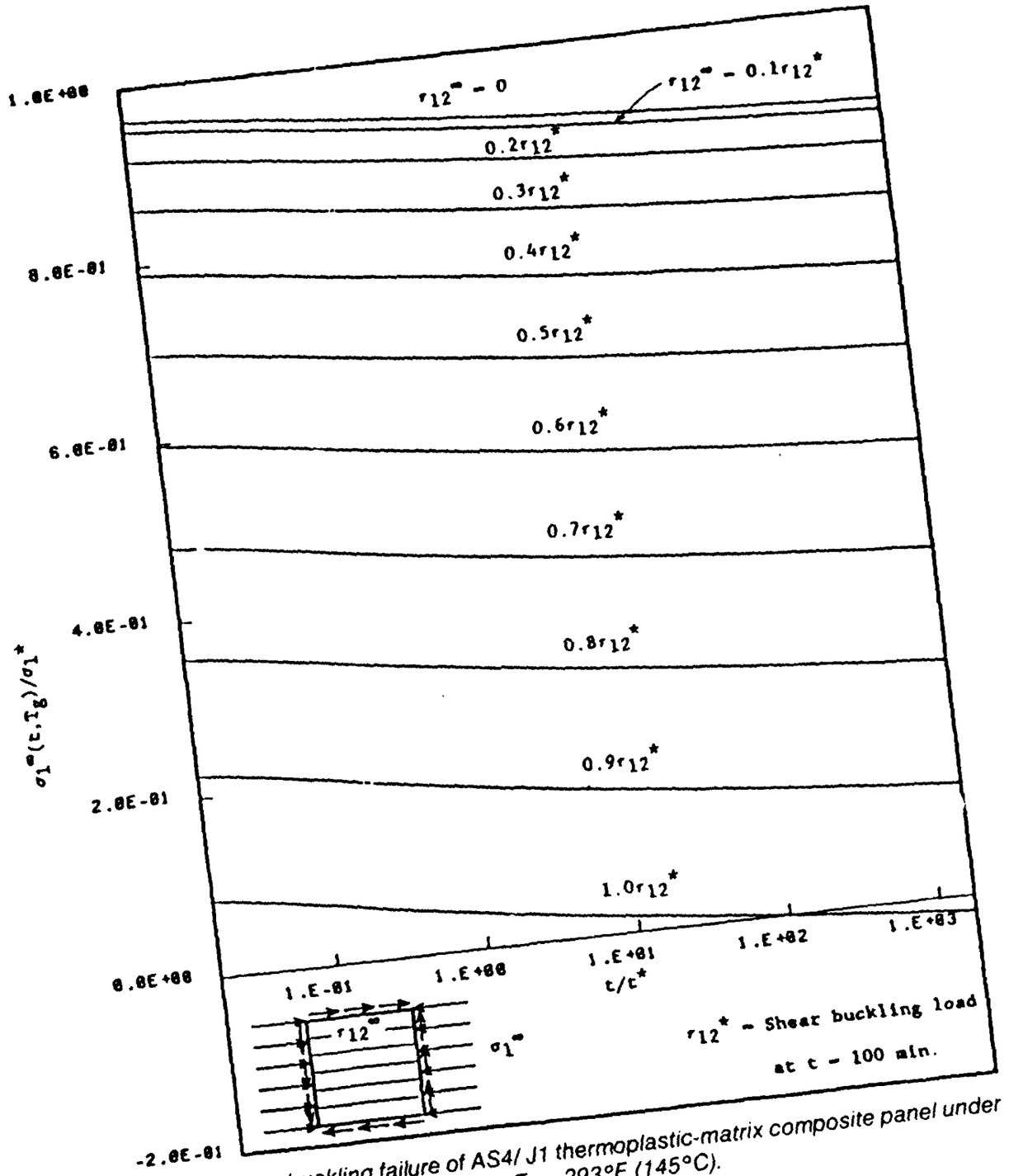

Figure 3-2-3. *Creep buckling failure of AS4/ J1 thermoplastic-matrix composite panel under combined axial compression and shear at T = 293°F (145°C).*

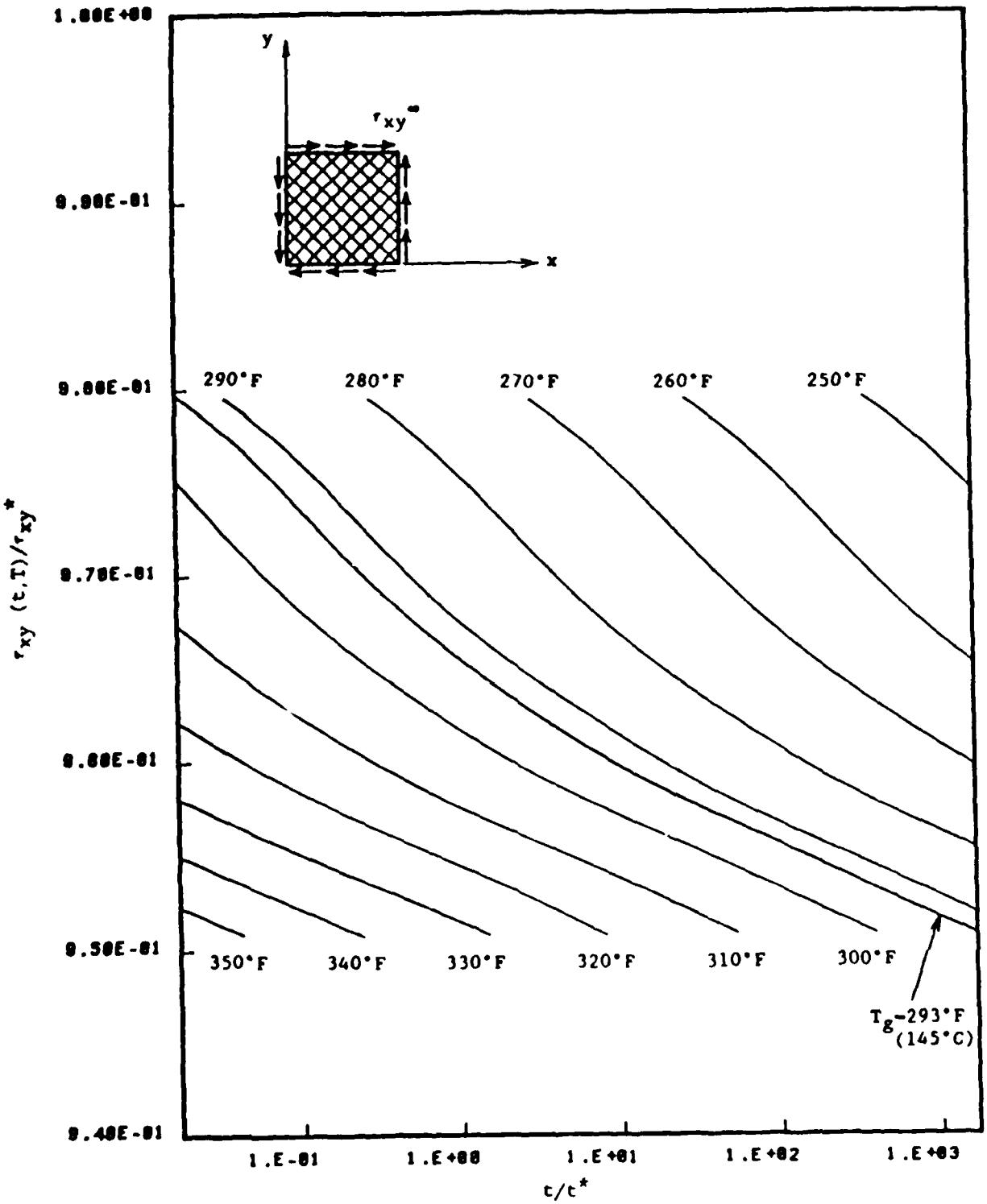

Figure 3-2-4. *Creep buckling failure of AS4/J1 thermoplastic-matrix composite angle ply under pure shear loading at various temperatures (t^{*} = 1 min.).*

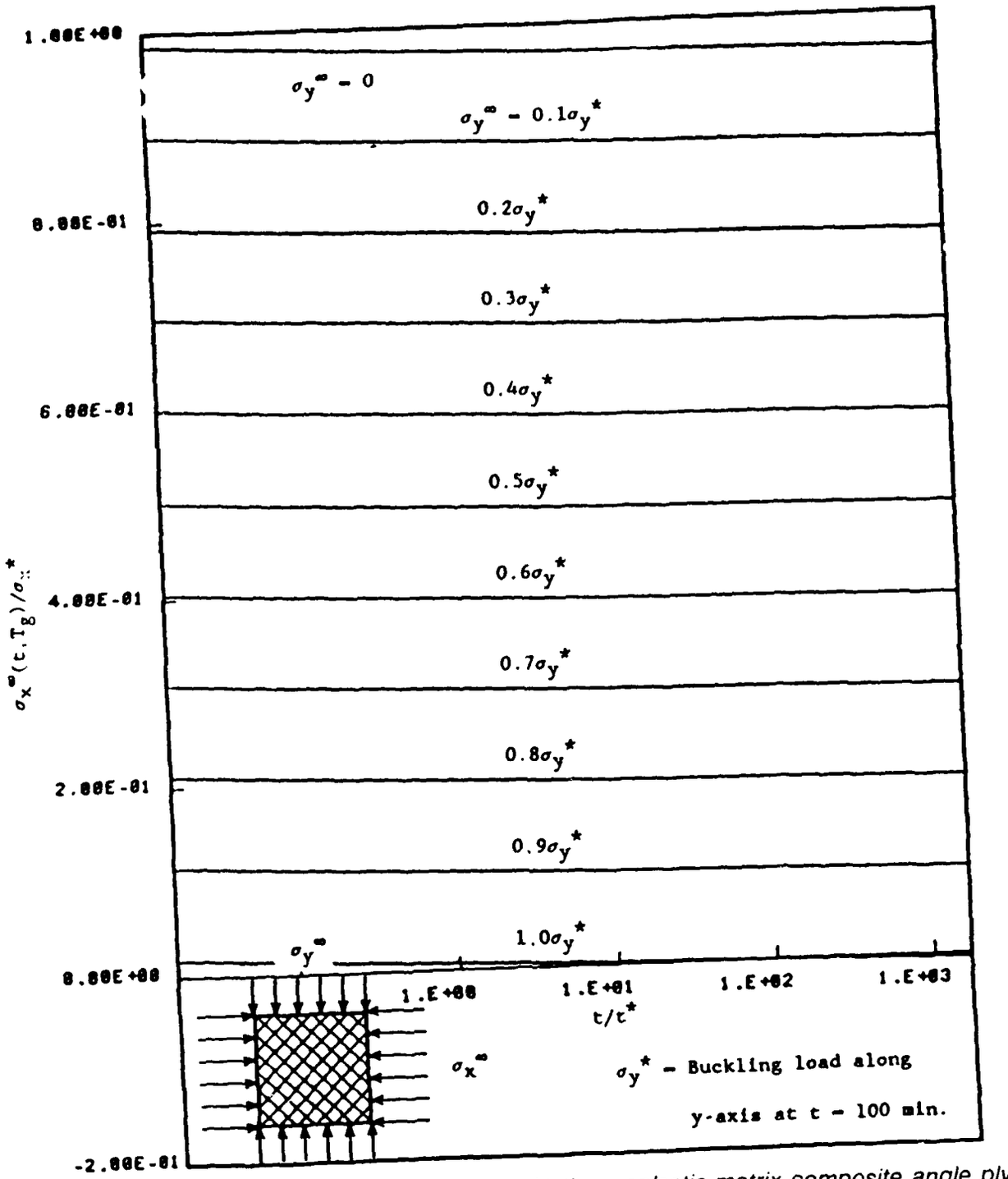

Figure 3-2-5. *Creep buckling failure of AS4/J1 thermoplastic-matrix composite angle ply under biaxial compression of various stress biaxiality ratios at T = 293°F (145°C).*

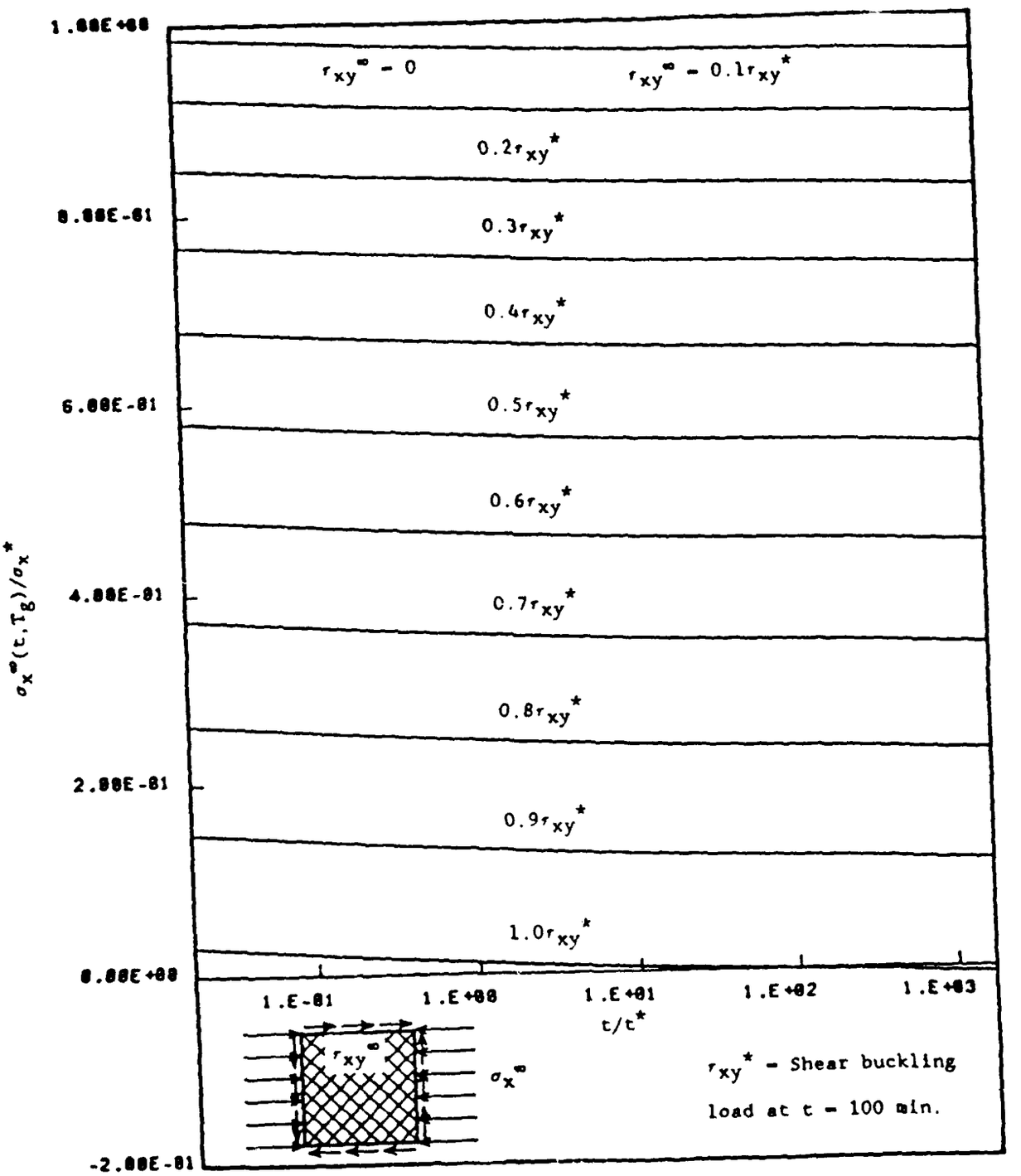

Figure 3-2-6. *Creep buckling failure of AS4/J1 thermoplastic-matrix composite angle ply under combined compression and shear at T = 293°F (145°C).*

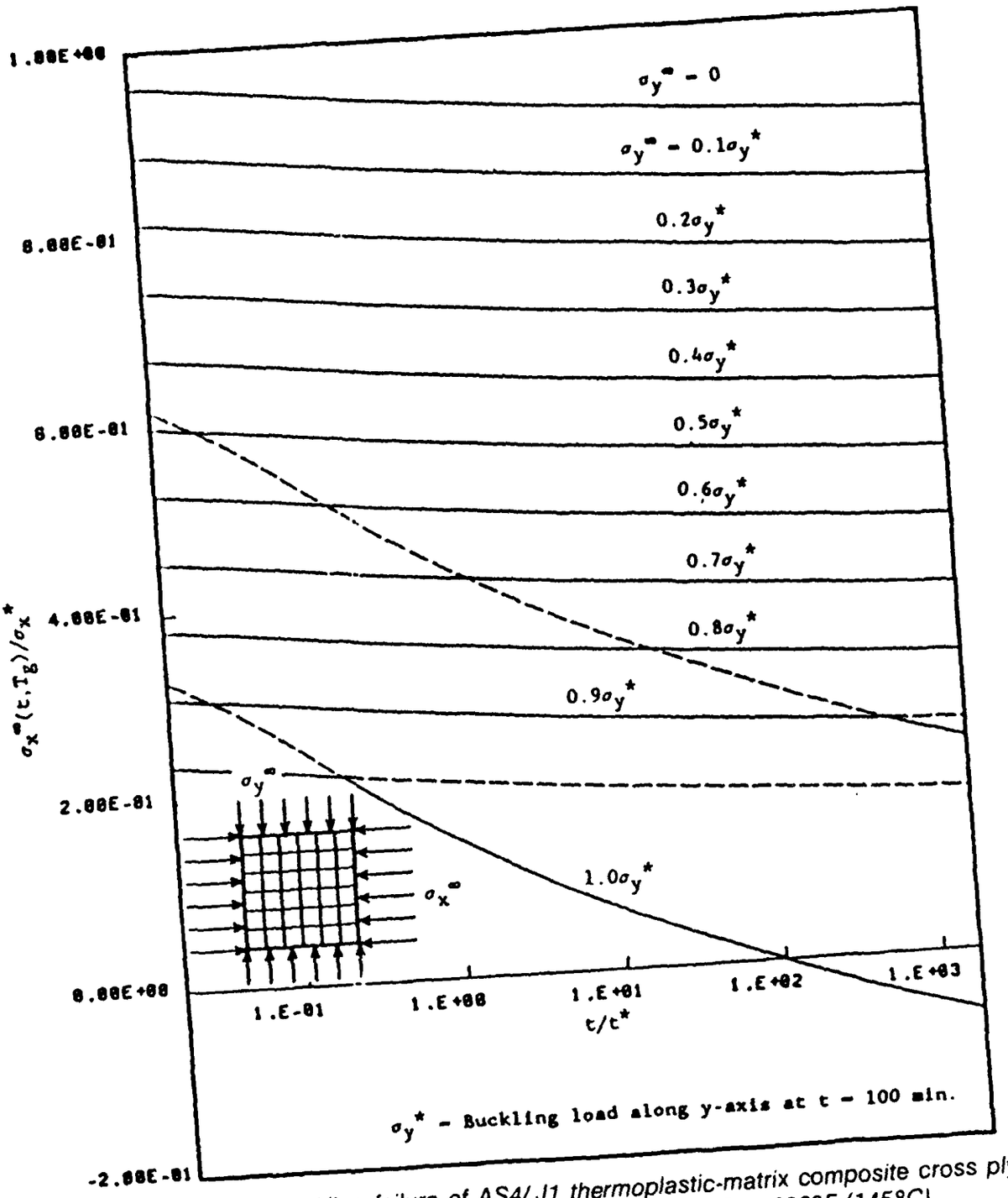

Figure 3-2-7. *Creep buckling failure of AS4/J1 thermoplastic-matrix composite cross ply under biaxial compression of various stress biaxiality ratios at T = 293°F (145°C).*

load σ_1^{∞} (t,T) is normalized with respect to σ_1^* which is the thermal elastic buckling load ($\sigma_1^* = 6.974$ ksi) at $T = 145°C$ under uniaxial compression. The σ_2^* in Figure 3-2-2 is the corresponding reference load of the same composite panel under uniaxial compression along the x_2 axis at $T = 145°C$ and $t = 100$ min.] The top solid line in Figure 3-2-2 is the creep buckling solution for $\sigma_2^{\infty} = 0$, i.e., a uniaxial compressive buckling in x_1 direction. The essential features of the biaxial creep buckling in Figure 3-2-2 are similar to those in a pure shear buckling case. At a given time t the introduction of σ_2^{∞} reduces the critical load σ_1^{∞} (t,T) and changes the mode shape. The cusps in Figure 3-2-2 made by two solutions corresponding to different mode shapes have significant physical importance. One is that they are the points at which both of the two mode shapes are admissible. The other is that sensitivity of the buckling time to the applied load σ_1^{∞} (t,T) changes near these points. The most significant difference from the elastic buckling is that in the case of elastic buckling, the mode shape change corresponds to the change in specific buckling characteristics of the structure. But in the case of creep buckling, the mode shape change occurs along with the creep buckling time.

3.2.c COMBINED AXIAL COMPRESSION AND SHEAR LOADING

In Figure 3-2-3, the relationship between the combined creep stresses σ_1^{∞} (t,T) and τ_{12}^{∞} (t,T) and the associated creep failure time t is shown. (Thermal elastic buckling loads σ_1^* are defined as that in the case 3.2.b.) The top solid line is identical to that in Figure 3-2-2, i.e., the uniaxial compressive creep buckling along the x_1 axis. Again, introduction of additional stress τ_{12}^* reduces the critical applied load at any buckling time. The shear stress τ_{12}^* is the reference shear stress which alone produces a 100 min. creep buckling time. In this loading case, the reduction is not uniform even without a mode shape change. A parametric study of the combined loading shows that the solution is much affected by the presence of the shear stress than that of transverse compression.

3.3 Creep Buckling of Thermoplastic Composite Laminates

3.3.a ANGLE-PLY COMPOSITE LAMINATES

i) Pure Shear Loading

The unique feature of the solution for an angle-ply thermoplastic AS4/J1 composite laminate is similar to that of the unidirectional composite panel. (τ_{xy}^* in Figure 3-2-4 is 23.97 ksi for the angle-ply composite laminate $T = 145°C$.) A comparison with Figure 3-2-1 shows that the creep buckling critical time is significantly extended for a given applied load. It is hard to observe directly from these figures because they are normalized by different factors. However, the creep buckling property or sensitivity of the creep buckling time to the applied load is also affected by the composite lamination variables.

ii) Biaxial Compression

The same changes can be seen in Figure 3-2-5. (σ_x^* in Figure 3-2-5 is 11.20

ksi.) The mode shape change observed in the case of the AS4/J1 unidirectional composite does not appear for the angle-ply composite laminate. Figure 3-2-8 also shows that mode shape does not change in a [45/−45/−45/45] composite laminate.

iii) Combined Axial Compression and Shear

Creep buckling resistance is improved similarly as the above two cases. The reduction of the critical load due to presence of additional shear stress at a given time is much more uniform compared to that of the unidirectional composite. Thus, the creep buckling time of the angle-ply laminate will not reduce so drastically as the case of the unidirectional composite by the presence of the shear stress.

3.3.b. CROSS-PLY COMPOSITE LAMINATES

In the case of cross-ply thermoplastic laminates, solutions for pure shear loading and combined axial compression and shear loading are exactly the same as those of the unidirectional composite. The reason is that the flexural rigidities in Equation (2-3-2a) are not changed in the case of $L_x = L_y$ but only those in Equation (2-3-2b) are affected. Consequently only the solutions which have the admissible roots form the Equation (2-3-2b) have different values. It should be noted that in the case of general rectangular laminates which have different L_x and L_y, all of the three solutions are different from those of unidirectional composites.

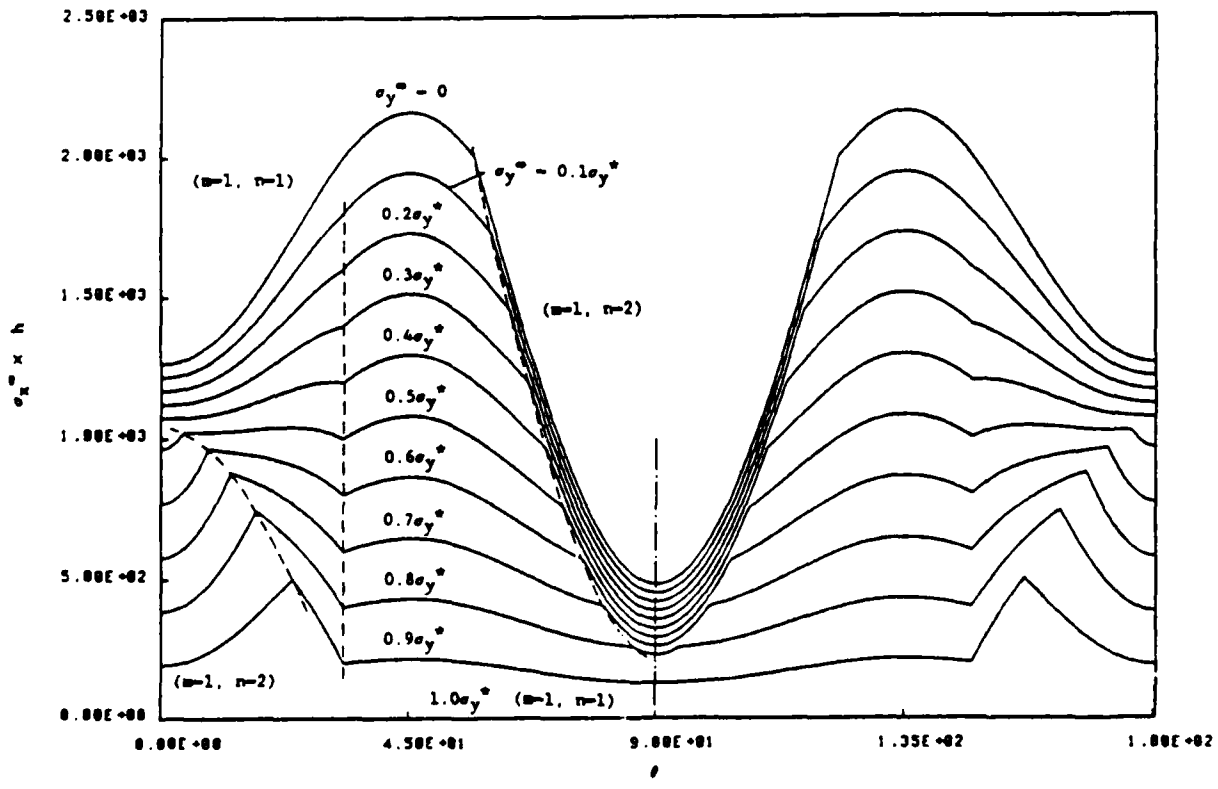

Figure 3-2-8. *Applied load which causes the 100 min. buckling time vs. angle θ of the composite angle ply $[\pm\theta]_s$ under biaxial compression at T = 293°F (145°C).*

Figure 3-2-7 shows that the admissible solution from Equation (2-3-2b) represents much improved creep buckling resistance so that the failure life increases significantly. Also, transition of the mode shape is much suppressed as compared with those of the unidirectional composites.

3.4 Mode Shape

Figure 3-2-8 shows variations of the applied load which causes the 100 min. buckling time in the biaxial compressive loading. The dotted line shows the admissible border between the two possible modes. Figure 3-2-9 shows the similar curves with Figure 3-2-8 in the case of the combined shear and compressive loading. The dotted lines show the borders along which the admissible solution changes between one from Equation (2-3-2a) and another from Equation (2-3-2b) that means the change of mode shape. The off-axis angle $\theta = 0°$ and $45°$ correspond to a unidirectional composite and angle-ply laminate respectively which were discussed previously.

Figure 3-2-10 and 3-2-11 show how the large fraction of the shear component can change the mode shapes drastically in the case of the combined axial compression and shear loading that is not seen in the other loading case.

4. CONCLUSIONS

Based on the analytical methods developed for studying the creep buckling failure of fiber composite laminates and the results obtained for the AS4/J1

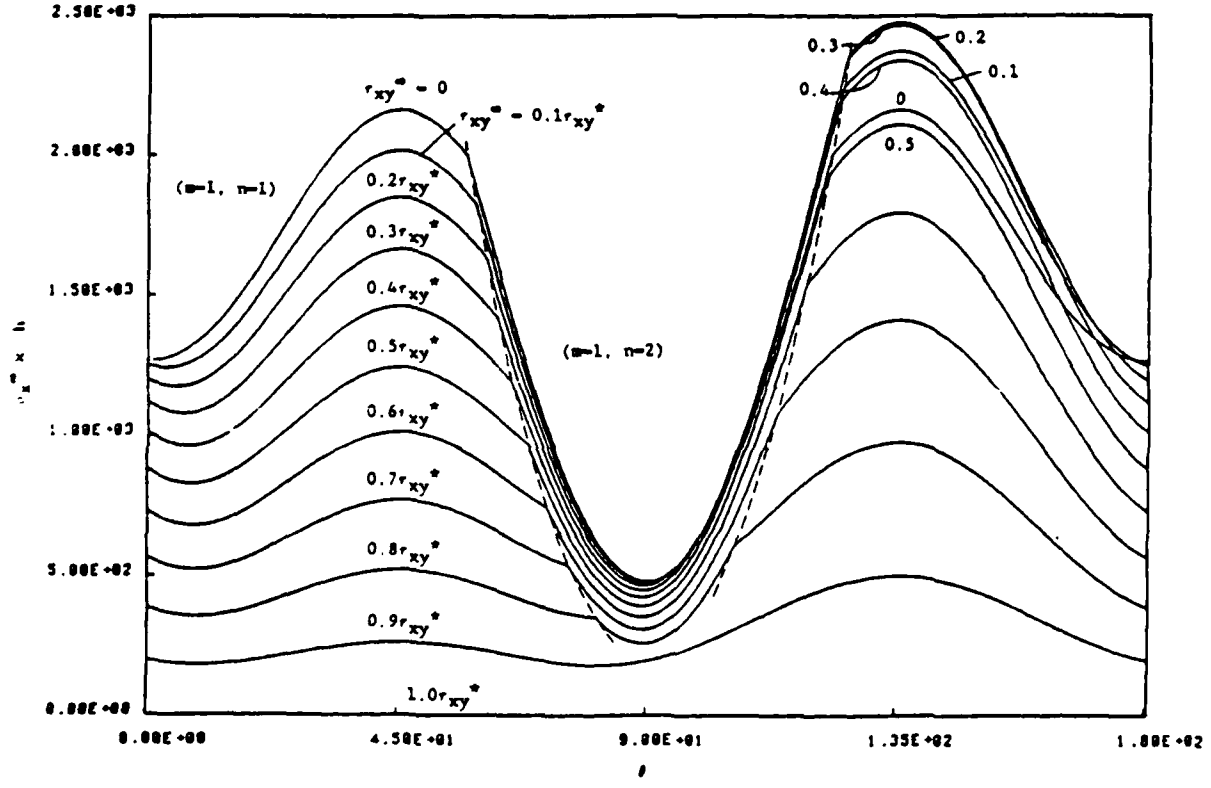

Figure 3-2-9. *Applied load which causes the 100 min. buckling time vs. angle θ of the composite angle ply $[\pm\theta]_s$ under combined axial compression and shear at T = 293°F (145°C).*

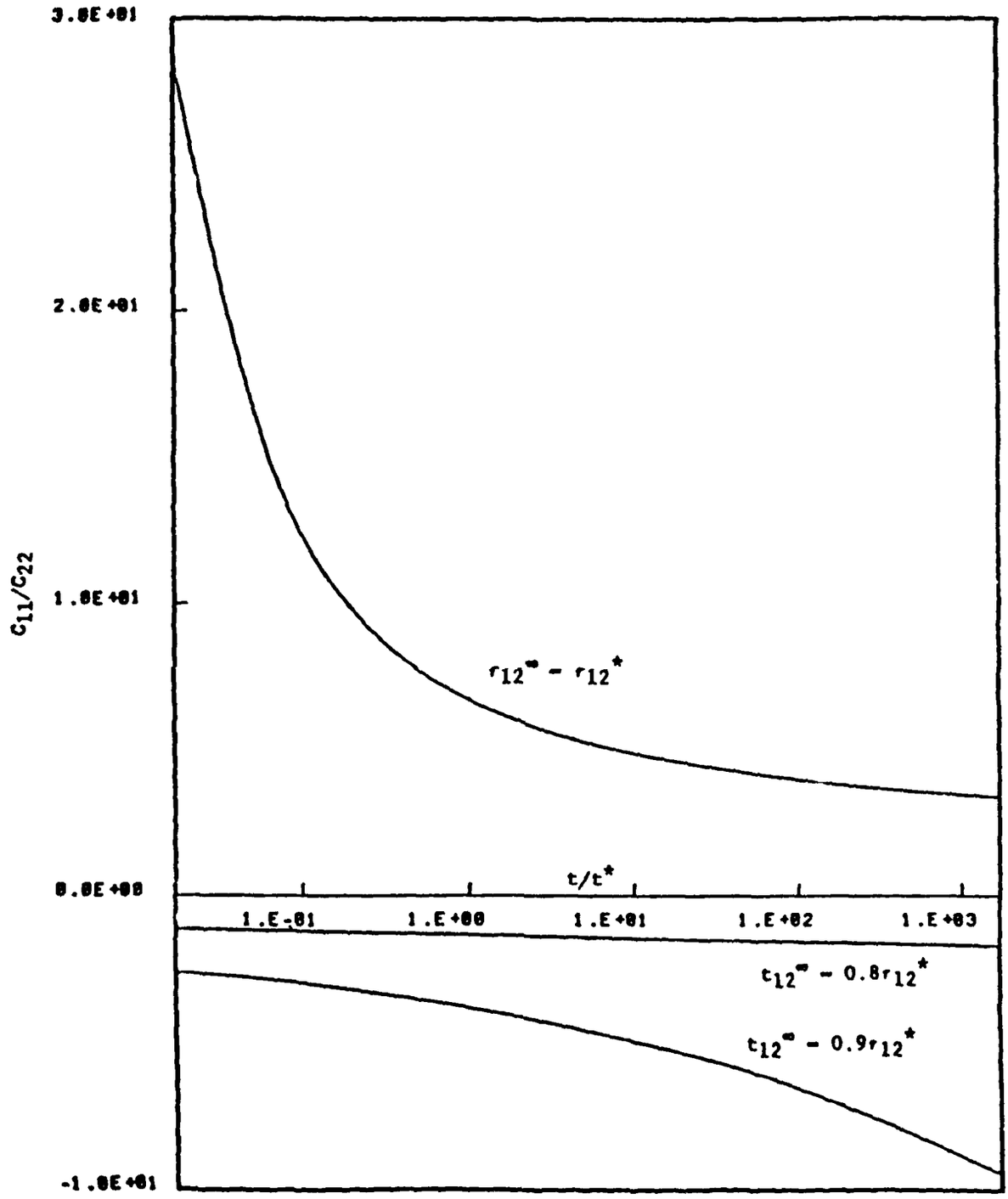

Figure 3-2-10. *Buckling mode of AS4/J1 thermoplastic-matrix composite undirectional panel under combined axial compression and shear at T = 293°F (145°C).*

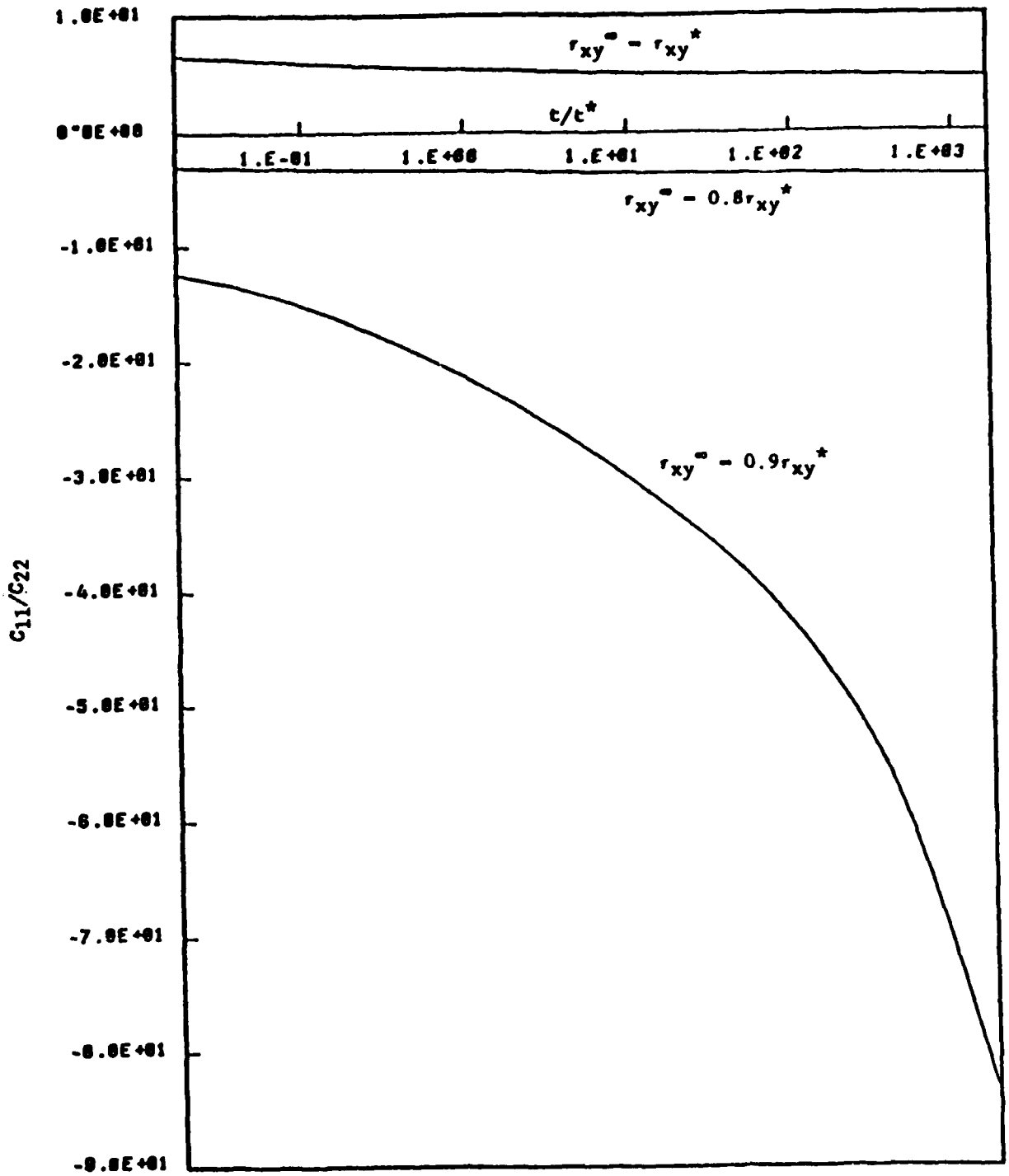

Figure 3-2-11. *Buckling mode of AS4/J1 thermoplastic-matrix composite angle ply under combined axial compression and shear at T = 293°F (145°C).*

thermoplastic-matrix composite panels under various loading modes in the elevated-temperature environment, the following conclusions can be made in this study:

1. The elevated-temperature anisotropic viscoelastic constitutive equations of the thermoplastic-matrix composite can be constructed, using the modified Prony series expansion with the aid of a sequential unconstrained minimization technique. The series solution for the composite time-temperature-dependent properties matches well with the experimental data in a range of five decade along the logarithmic scale.
2. The elevated-temperature viscoelastic creep buckling of the composite panels is analyzed successfully by the use of the well-known Galerkin's method and the inverse Laplace transformation technique. At a specific time creep buckling loads of a thermoplastic composite laminate panel are determined at various temperatures and under various combinations of biaxial loading modes.
3. The creep buckling failure time of a thermoplastic composite panel under a given load (e.g., uniaxial, shear or biaxial) is determined by a time-dependent bifurcation analysis of the characteristic equations in conjuction with the inverse Laplace transformation.
4. At a given temperature, the shear creep buckling load of the unidirectional AS4/J1 thermoplastic-matrix composite appears to decrease more rapidly with time than that of an angle-ply $[\pm 45°]_s$ composite laminate. As anticipated, the symmetric angle-ply $[\pm 45°]_s$ laminate has a better resistance to elevated temperature shear creep deformation and failure.
5. The elevated-temperature creep buckling resistance of a composite laminate panel is strongly affected by the biaxial compressive loading. The introduction of σ_2^∞ in a compressively loaded (σ_1^∞) composite plate significantly reduces the axial creep buckling resistance in all three cases studied (i.e., pure shear, biaxial compression, and combined shear and compression). It also changes the buckling shape modes in the cases of uniaxial composite and cross-ply composite laminates. However, this phenomenon is not observed in the $[\pm 45°]_s$ laminate at any temperatures.
6. The elevated-temperature creep buckling strength of a composite laminate panel is also affected by the combined axial compression and shear loading. The additional shear introduced to the axially loaded composite significantly reduces the composite panel load bearing capacity. However, in both the unidirectional composite and the $[\pm 45°]_s$ composite, mode shape changes at any temperatures and load combinations are not observed.
7. In biaxially compressed thermoplastic angle-ply composite laminates (i.e., $\sigma_1^\infty \neq 0$, $\sigma_2^\infty \neq 0$), fiber orientations affect not only the creep buckling load level but also the mode shape associated with the failure. For example, in a $[\theta/-\theta/-\theta/\theta]$ AS4/J1 composite laminate at 145°C subjected various combinations of $\sigma_1^\infty/\sigma_2^\infty$, the dominant mode shape during creep buckling of the laminate with $\theta < 33°$ is $m = 1$ and $n = 1$, whereas the $\theta > 33°$ the buckling mode shape is $m = 1$, $n = 2$ under any combination of σ_1^∞ and σ_2^∞.

8. In the case of combined compression and shear, fiber orientation does not affect the mode shape change significantly but the load level. Due to the presence of the shear, symmetry of the characteristics in which the load level is affected by the fiber orientation along $\theta = 90°$ is lost.

APPENDIX 1: SEQUENTIAL UNCONSTRAINED MINIMIZATION TECHNIQUE (SUMT)

To express the experimental data of the anisotropic composite properties by proper analytical expressions, a sequential unconstrained minimization technique [9] which is one of the commonly used optimization techniques is employed instead of the conventional Prony expansion method [18]. In the present study, 15 terms are used for the creep compliances and 13 terms for the time-dependent Poisson's ratio. The number of the terms used is determined by two factors which conflict with each other. An accurate solution in the desired time range requires many terms but, on the contrary, most of the terms are used to fit the end portions of the curve. And very often the resolutions are lost because of the limit of the precision in the calculation.

The original objective function f for the present problem is

$$f = \sum_{i=1}^{N} \{F_{ex}(t_i) - F_{mp}(t_i)\}^2 \tag{A-1-1}$$

where

$F_{ex}(t_i)$ = experimental data for the compliances or the Poisson's ratio at $t = t_i$

$F_{mp}(t_i)$ = the compliance function or Poisson's ratio calculated by the modified Prony series solution

The constraint conditions should be expressed as follows to be used with SUMT method:

$$g_i > 0 \qquad (i = 1, N_c \;\; ; \;\; N_c\text{: Number of constraint conditions}) \tag{A-1-2}$$

For the compliances for example,

$$\beta_k(T) > 0 \tag{A-1-3a}$$

where β_k is the new variable introduced for convenience instead of μ_k. The relations between them are

$$\beta_k(T) = \exp[\mu_k(T)] \tag{A-1-4}$$

Besides this essential constraint condition, two additional constraint conditions are necessary due to the reasons mentioned previously:

$$-C_{ij}^{(k)}(T) > 0 \qquad (k = 1,n) \tag{A-1-3b}$$

$$1 - \beta_k(T) > 0 \qquad (k = 1,n) \tag{A-1-3c}$$

Similar conditions are necessary for the constants in the expression for Poisson's ratio.

A number of these constraint conditions can be automatically satisfied by modifying the objective function as

$$u = f + \sum_{i=1}^{Nc} (r_i/g_i) \tag{A-1-5}$$

The summation term is the penalty term introduced instead of the constraint conditions. By reducing r_i gradually to zero during the iteration of the conventional steepest descent method [9], the optimum solution for u can be obtained which is actually the same solution for f with all of the constraint conditions.

The SUMT method resolves the complicacy to handle a number of constraint conditions but still difficulties remain in selecting proper initial values and in reducing the magnitude of the coefficients of the penalty terms appropriately which are at present solved by trial and error.

APPENDIX 2

The explicit forms for the flexural rigidities for the angle-ply laminates are:

$$D_{xx} = \frac{2t^3}{3(1 - \nu_{12}\nu_{21})} [E_{22} \sin^4 \theta + 2\{\nu_{21}E_{11} + 2(1 - \nu_{12}\nu_{21})G_{66}\} \sin^2 \theta \cos^2 \theta + E_{11} \cos^4 \theta]$$

$$D_{yy} = \frac{2t^3}{3(1 - \nu_{12}\nu_{21})} [E_{11} \sin^4 \theta + 2\{\nu_{21}E_{11} + 2(1 - \nu_{12}\nu_{21})G_{66}\} \sin^2 \theta \cos^2 \theta + E_{22} \cos^4 \theta]$$

$$D_{xy} = \frac{2t^3}{3(1 - \nu_{12}\nu_{21})} [\nu_{21}E_{11}(\sigma_t\nu^4\theta + \cos^4 \theta) + \{\nu_{21}E_{11} - 4(1 - \nu_{12}\nu_{21})G_{66}\} \sin^2 \theta \cos^2 \theta]$$

$$D_{ss} = \frac{2t^3}{3(1 - \nu_{12}\nu_{21})} [(E_{22} + E_{11} - 2\nu_{21}) \sin^2 \theta \cos^2 \theta + G_{66}(\cos^2 \theta - \sin^2 \theta)^2]$$

$$D_{xs} = \frac{-t^3}{2(1 - \nu_{12}\nu_{21})} [E_{22} \cos \theta \sin^3 \theta - E_{11} \cos^3 \theta \sin \theta + \{\nu_{21}E_{11} + 2(1 - \nu_{12}\nu_{21})G_{66}\} \sin^\theta \cos^\theta (\sin^2 \theta - \cos^2 \theta)]$$

$$D_{ys} = \frac{-t^3}{2(1 - \nu_{12}\nu_{21})} [E_{22} \sin \theta \cos^3 \theta - E_{11} \sin^3 \theta \cos \theta + \{\nu_{21}E_{11} + 2(1 - \nu_{12}\nu_{21})G_{66}\} \sin^\theta \cos^\theta (\sin^2 \theta - \cos^2 \theta)]$$

APPENDIX 3

The expanded form of Equation (2-3-2a) for the angle-ply laminates to solve for the applied loads is:

$$
\begin{aligned}
&(I_{0022} - 2I_{1122} + I_{2222})N_{xy}^2 + (20/3)\pi^2 + 2c^3)\{A_1(I_{0012} - I_{1112}) - A_{22}(I_{0022} \\
&\quad - I_{1122}) + A_3(I_{0122} - I_{1222}) + A_4(I_{0021} - 2I_{1112} + I_{2221})\}N_{xy} \\
&\quad + 16\pi^4\{(2/3)t^3(-1 + 2c^3)\}^2\{A_1^2 I_{0002} + A_2^2 I_{0022} + A_3^2 I_{0222} \\
&\quad + A_4^2(I_{0020} + 2I_{1120} - 2I_{1120}) - 2A_1A_2I_{0012} + 2A_1A_3I_{0012} \\
&\quad + 2A_1A_4(I_{0011} - I_{1111}) - 2A_2A_3I_{0122} - 2A_2A_4(I_{0021} \\
&\quad - I_{1121}) + A_3A_4(I_{0121} - I_{1221})\} - \{(3/16)L_xL_yt^3\pi^4\}^2[A_5^2 I_{0002} \\
&\quad + A_6^2 I_{0022} + A_7^2 I_{0222} + A_8^2(I_{0020} - 2I_{1120} + I_{2220}) \\
&\quad + 2A_5A_6I_{0012} + 2A_5A_7I_{0112} + 2A_5A_8(I_{0011} + I_{1111}) \\
&\quad + 2A_6A_7I_{0122} + 2A_6A_8(I_{0021} - I_{1121}) + 2A_7A_8(I_{0121} - I_{1221})] \\
&\quad + \{(10/3)t^3\}\pi^2[A_5(I_{0012} - I_{1112})\, A_6(I_{0022} - I_{1122}) \\
&\quad + A_7(I_{0122} - I_{1222}) + A_8(I_{0021} - 2I_{1121} + I_{2221})](N_x/L_x^2 - N_y/L_y^2)^2 \\
&\quad - (I_{0022} - 2I_{1122} + I_{2222})(N_x/L_x^2 - N_y/L_y^2 = 0 \qquad \text{(A-3-1)}
\end{aligned}
$$

where

$$A_1 = \sin^\theta \cos^\theta(\sin^2\theta/L_x^2 + \cos^2\theta/L_y^2)$$

$$A_2 = \sin^\theta \cos^\theta(\cos^2\theta/L_x^2 + \sin^2\theta/L_y^2)E_{11}$$

$$A_3 = \sin^\theta \cos^\theta(\cos^2\theta - \sin^2\theta)(1/L_x^2 - 1/L_7^2)E_{11}$$

$$A_4 = 2\sin^\theta \cos^\theta(\cos^2\theta - \sin^2\theta)(1/L_x^2 - 1/L_7^2)$$

$$A_5 = \sin^4\theta/L_x^4 + 6\sigma_{l\nu}{}^2\theta\cos^2\theta/L_x^2L_y^2 + \cos^4\theta/L_y^2$$

$$A_6 = (\sin^4\theta/L_x^4 + 6\sigma_{l\nu}{}^2\theta\cos^2\theta/L_x^2L_y^2 + \cos^4\theta/L_y^2)E_{11}$$

$$A_7 = 2E_{11}\cos^2\theta\sin^2\theta/L_x^4 + 2(\cos^4\theta + \sin^4\theta - 4\cos^2\theta\sin^2\theta) \times E_{11}/(L_xL_y)^2 + 2E_{11}\cos^2\theta\sin^2\theta/L_y^4$$

$$A_8 = 4\cos^2\theta\sin^2\theta/L_x^4 + 4(\cos^4\theta + \sin^4\theta)/(L_xL_y)^2 + 4\cos^2\theta\sin^2\theta/L_y^4 \tag{A-3-2}$$

The expanded form for Equation (2-3-2b) is shown as Equation (2-3-4). The explicit form of B_1 to B_{18} are:

$$\begin{aligned}
B_1 &= \sin^8\theta I_{0002} + 4\sin^4\theta\cos^4\theta\{E_{11}^2 I_{0222} + 4E_{11}(I_{0121} + I_{1221}) + 4(I_{0020} \\
&\quad - 2I_{1120} + I_{2220})\} + E_{11}^2\cos^8\theta I_{0022} + 4\cos^2\theta\sin^6\theta[E_{11}I_{0112} + 2I_{0011} \\
&\quad - 2I_{1111}] + 4E_{11}\cos^6\theta\sin^2\theta[E_{11}I_{0122} + 2I_{0021} - 2I_{1121}] \\
&\quad + 2E_x\cos^4\sin^4\theta I_{0012} \\
B_2 &= \sin^4\theta(\sin^4\theta + \cos^4\theta)E_{11}I_{0112} + \sin^6\theta\cos^2\theta[E_{11}I_{0012} + I_{0002} \\
&\quad - 4I(I_{0011} - I_{1111})] + 2\cos^2\theta\sin^2\theta(\sin^4\theta + \cos^4\theta)E_{11}[E_{11}I_{0022} \\
&\quad + 2(I_{0121} - I_{1221})] + 2\sin^4\theta\cos^4\theta[E_{11}^2 I_{0122} + E_{11}I_{0112} - 4E_{11}(I_{0121} \\
&\quad - I_{1221}) + 2E_{11}(I_{0021} - I_{1121}) + 2(I_{0011} - I_{1111}) - 8(I_{0020} - 2I_{1120} \\
&\quad + I_{2220})] + \cos^4\theta(\sin^4\theta + \cos^4\theta(E_{11}^2 I_{0122} + \sin^2\theta\cos^6\theta E_{11}[E_{11}I_{0022} \\
&\quad + I_{0012} - 4(I_{0021} - I_{1121})] \\
B_3 &= \cos^2\theta\sin^6\theta(E_{11}I_{0012} + I_{0002} - 2IE_{11}I_{0112}) + \sin^4\theta(\cos^2\theta \\
&\quad - \sin^2\theta)^2(I_{0011} + I_{1111}) + 2\cos^4\theta\sin^4\theta[E_{11}^2 I_{0122} + E_{11}I_{0112} \\
&\quad - 2E_{11}^2 I_{0222} + 2E_{11}(I_{0021} - I_{1121}) + 2(I_{0011} - I_{1111}) - 4E_{11}(I_{0121} \\
&\quad - I_{1221})] + 2\cos^2\theta\sin^2\theta(\cos^2\theta - \sin^2\theta)^2[E_{11}(I_{0121} - I_{1221}) \\
&\quad + 2(I_{0020} - 2I_{1120} + I_{2220})] + \cos^6\theta\sin^2\theta E_{11}(E_{11}I_{0022} + I_{0012} \\
&\quad - 2E_{11}I_{0122}) + E_{11}\cos^4\theta(\cos^2\theta - \sin^2\theta)^2(I_{0021} - I_{1121}) \\
B_4 &= \sin^8\theta E_{11}I_{0012} + 2\cos^2\theta\sin^6\theta(E_{11}I_{0012} + 2I_{0011} - 2I_{1111}) \\
&\quad + \sin^4\theta\cos^4\theta I_{0002} + 2\cos^2\theta\sin^6\theta E_{11}(E_{11}I_{0122} + 2I_{0021} - 2I_{1121}) \\
&\quad + 4\sin^4\theta\cos^4\theta[E_x^2 I_{0222} + 4E_x(I_{0121} - I_{1221}) + 4(I_{0020} - 2I_{1120} \\
&\quad + I_{2220})] + 2\cos^6\theta\sin^2\theta(E_{11}I_{0112} + 2I_{0011} - 2I_{1111})
\end{aligned}$$

$$+ \sin^4\theta \cos^4\theta E_{11} I_{0022} + 2\cos^6\theta \sin^2\theta E_{11}(E_{11} I_{0122} + 2I_{0021} - 2I_{1121})$$
$$+ \cos^8\theta E_{11} I_{0012}$$

$$B_5 = (\sin^4\theta + \cos^4\theta)E_{11}^2 I_{0222} + 2\sin^2\theta\cos^2\theta(\sin^4\theta + \cos^4\theta)[E_{11}^2 I_{0122}$$
$$+ E_{11} I_{0112} - 4E_{11}(I_{0121} - I_{1221}) + \sin^4\theta\cos^4\theta[E_{11}^2 I_{0022} + I_{0002}$$
$$- 16(I_{0020} - 2I_{1120} + I_{2220})2E_{11} I_{0012} - 8(I_{0011} - I_{1111}) - 8E_{11}(I_{0021}$$
$$- I_{1121})]$$

$$B_6 = +2E_{11}\, sin^2\theta\cos^2\theta(\sin^4\theta + \cos^4\theta)(E_{11} I_{0122} + I_{0112} - 2E_{11} I_{0222})$$
$$+ E_{11}(\sin^2\theta - \cos^2\theta)^2(\sin^4\theta + \cos^4\theta)(I_{0121} - I_{1221})$$
$$+ \sin^4\theta\cos^4\theta[E_{11}^2 I_{0022} + 2E_{11} I_{0012} + I_{0002} - 2E_{11}^2 I_{0122} - 2E_{11\,0122}$$
$$- 4E_{11}(I_{0021} - I_{1121}) - 4(I_{0011} - I_{1111}) + 8E_{11}(I_{0121} - I_{1221})]$$
$$+ \cos^2\theta\sin^2\theta(\cos^2\theta - \sin^2\theta)^2[E_{11}(I_{0021} - I_{1121}) + (I_{0011} - I_{1111})$$
$$- 4(I_{0020} - 2I_{1120} + I_{2220})]$$

$$B_7 = +\sin^4\theta\cos^4\theta[E_{11}^2 I_{0022} + 2E_{11} I_{0012} + I_{0002} + 4E_{11}^2 I_{0222}$$
$$- 4E_{11} I_{0112} - 4E_{11}^2 I_{0122}] + \cos^2\theta\sin^2\theta(\cos^2\theta - \sin^2\theta)^2[E_{11}(I_{0021}$$
$$- I_{1121}) + (I_{0011} - I_{1111}) - 2E_{11}(I_{0121} - I_{1221})] + (\cos^2\theta$$
$$- \sin^2\theta)^4(I_{0020} - 2I_{1120} + I_{2220})$$

$$B_8 = \sin^4\theta(\sin^4\theta + \cos^4\theta)E_{11}^2 I_{0122} + E_{11}\sin^6\theta\cos^2\theta[E_{11} I_{0022} + I_{0012}$$
$$- 4(I_{0021} - I_{1121})] + 2\cos^2\theta\sin^2\theta(\sin^4\theta + \cos^4\theta)E_{11}[E_{11} I_{0222}$$
$$+ 2(I_{0121} - I_{1221})] + 2\sin^4\theta\cos^4\theta[E_{11}^2 I_{0122} + E_{11} I_{0112}$$
$$- 4E_{11}(I_{0121} - I_{1221}) + 2E_{11}(I_{0021} - I_{1121}) + 2(I_{0011} - I_{1111}) - 8(I_{0020}$$
$$- 2I_{1120} + I_{2220})] + \cos^4\theta(\sin^4\theta + \cos^4\theta)E_{11} I_{0112}$$
$$+ \sin^2\theta\cos^6\theta[E_{11} I_{0012} + I_{0002} - 4(I_{0011} - I_{1111})]$$

$$B_9 = \cos^2\theta\sin^6\theta E_{11}(E_{11} I_{0002} + I_{0012} - 2IE_{11} I_{0122}) + \sin^4\theta(\cos^2\theta$$

$$- \sin^2\theta)^2 E_{11}(I_{0021} - I_{1121}) + 2\cos^4\theta \sin^4\theta[E_{11}^2 I_{0122} + E_{11} I_{0012}$$

$$- 2E_{11}^2 I_{0222} + 2E_{11}(I_{0021} - I_{1121}) + 2(I_{0011} - I_{1111}) - 4E_{11}(I_{0121}$$

$$- I_{1221})] + 2\cos^2\theta \sin^2\theta(\cos^2\theta - \sin^2\theta)^2[E_{11}(I_{0121} - I_{1221})$$

$$+ 2(I_{0020} - 2I_{1120} + I_{2220})] - \cos^6\theta \sin^2\theta(E_{11} I_{0012} + I_{0002}$$

$$- 2E_{11} I_{0112}) + \cos^4\theta(\cos^2\theta - \sin^2\theta)^2(I_{0011} - I_{1111})$$

$$B_{10} = \sin^8\theta E_{11}^2 I_{0022} + 4\sin^4\theta \cos^4\theta[E_{11}^2 I_{0222} + 4E_{11}(I_{0121} - I_{1221})$$

$$+ 4(I_{0020} - 2I_{1120} + I_{2220})] + \cos^8\theta I_{0022} + 4\cos^2\theta \sin^6\theta[E_{11}^2 I_{0122}$$

$$+ 2E_{11}(I_{0021} - I_{1121})] + 4\cos^6\theta \sin^2\theta[E_x I_{0112} + 2I_{0011} - 2I_{111}]$$

$$+ 2E_{11}\cos^4\theta \sin^4\theta I_{0012}$$

$$B_{11} = (1/L_x^4)[\sin^4\theta(I_{0012} - I_{1112}) + 2\cos^2\theta \sin^2\theta E_{11}(I_{0112} - I_{1122})$$

$$+ 4\cos^2\theta \sin^2\theta(I_{0021} - 2I_{1121} + I_{2221}) + E_{11}\cos^4\theta(I_{0022} - I_{1122})]$$

$$+ [8/(L_x^2 L_y^2)][(\sin^4\theta + \cos^4\theta)E_{11}(I_{0122} - I_{1222})$$

$$+ 2\cos^2\theta \sin^2\theta E_{11}(I_{0112} - I_{1122}) - 4\cos^2\theta \sin^2\theta(I_{0021} - 2I_{1121}$$

$$+ I_{2221})] + [16/(L_x^2 L_y^2)][\cos^2\theta \sin^2\theta E_{11}(I_{0022} - I_{1122})$$

$$+ \cos^2\theta \sin^2\theta(I_{0112} - I_{1122}) - 2\cos^2\theta \sin^2\theta E_{11}(I_{0122} - I_{1222})$$

$$+ (\cos^2\theta - \sin^2\theta)^2(I_{0021} - 2I_{1121} + I_{2221})] + (16/L_y^4)[\sin^4\theta E_{11}(I_{0022}$$

$$- I_{1122}) + \cos^4\theta(I_{0012} - I_{1112}) + 2\cos^2\theta \sin^2\theta E_{11}(I_{0122} - I_{1222})$$

$$+ 4\cos^2\theta \sin^2\theta(I_{0021} - 2I_{1121} + I_{2221})]$$

$$B_{12} = (16/L_x^4)[\sin^4\theta(I_{0012} - I_{1112}) + 2\cos^2\theta \sin^2\theta E_{11}(I_{0112} - I_{1122})$$

$$+ 4\cos^2\theta \sin^2\theta(I_{0021} - 2I_{1121} + I_{2221}) + E_{11}\cos^4\theta(I_{0022} - I_{1122})]$$

$$+ [8/(L_x^2 L_y^2)][(\sin^4\theta + \cos^4\theta)E_{11}(I_{0122} - I_{1222})$$

$$+ 2\cos^2\theta \sin^2\theta E_{11}(I_{0112} - I_{1122}) - 4\cos^2\theta \sin^2\theta(I_{0021} - 2I_{1121}$$

$$+ I_{2221})] + [16/(L_x^2 L_y^2)][\cos^2\theta \sin^2\theta E_{11}(I_{0022} - I_{1122})$$

$$+ \cos^2\theta \sin^2\theta(I_{0112} - I_{1122}) - 2\cos^2\theta \sin^2\theta E_{11}(I_{0122} - I_{1222})$$

$$+ (\cos^2\theta - \sin^2\theta)^2(I_{0021} - 2I_{1121} + I_{2221})] + (1/L_y^4)[\sin^4\theta E_{11}(I_{0022}$$

$$- I_{1122}) + \cos^4\theta(I_{0012} - I_{1112}) + 2\cos^2\theta \sin^2\theta E_{11}(I_{0122} - I_{1222})$$

$$+ 4\cos^2\theta \sin^2\theta(I_{0021} - 2I_{1121} + I_{2221})]$$

$$B_{13} = I_{0022} - 2I_{1122} + I_{2222}$$

$$B_{14} = \cos^2\theta \sin^6\theta I_{0002} + \cos^6\theta \sin^2\theta E_{11}^2 I_{0022} + \cos^2\theta \sin^2\theta(\cos^2\theta$$

$$- \sin^2\theta)^2(E_{11}^2 I_{0222} + 4E_{11}(I_{0121} - I_{1221}) + 4(I_{0020} - 2I_{1120} + I_{2220})]$$

$$- 2\cos^4\theta \sin^4\theta E_{11} I_{0012} - 2\cos^4\theta \sin^2\theta(\text{cis}^2\theta - \sin^2\theta)E_{11}[E_{11} I_{0122}$$

$$+ 2(I_{0021} - I_{1121})] + 2\cos^2\theta \sin^4\theta(\text{cis}^2\theta - \sin^2\theta)E_{11}[E_{11} I_{0122}$$

$$+ 2(I_{0021} - I_{1121})]$$

$$B_{15} = \cos^6\theta \sin^2\theta I_{0002} + \cos^2\theta \sin^6\theta E_{11}^2 I_{0022} + \cos^2\theta \sin^2\theta(\cos^2\theta$$

$$- \sin^2\theta)^2[E_{11}^2 I_{0222} + 4E_{11}(I_{0121} - I_{1221}) + 4(I_{0020} - 2I_{1120} + I_{2220})]$$

$$- 2\cos^4\theta \sin^4\theta E_{11} I_{0012} - 2\cos^2\theta \sin^4\theta(\text{cis}^2\theta - \sin^2\theta)E_{11}[E_{11} I_{0122}$$

$$+ 2(I_{0021} - I_{1121})] + 2\cos^4\theta \sin^2\theta(\text{cis}^2\theta - \sin^2\theta)E_{11}[E_{11} I_{0122}$$

$$+ 2(I_{0021} - I_{1121})]$$

$$B_{16} = \cos^4\theta \sin^4\theta I_{0002} - \cos^2\theta \sin^2\theta(\cos^2\theta + \sin^2\theta)I_{0012}$$

$$+ \cos^4\theta \sin^4\theta E_{11} I_{0022} + (\cos^3\theta \sin\theta - \cos\theta \sin^3\theta)\cos\theta \sin\theta(\cos^2\theta$$

$$- \sin^2\theta)[E_{11}^2 I_{0122} + 2E_{11}(I_{0021} - I_{1121}) + E_{11} I_{0112} + 2(I_{0011} - I_{1111})]$$

$$- \cos^2\theta \sin^2\theta(\cos^2\theta - \sin^2\theta)^2[E_{11}^2 I_{0222} + 4E_{11}(I_{0121} - I_{1221})$$

$$+ 4(I_{0020} - 2I_{1120} + I_{2220})]$$

$$B_{17} = (4/L_x^2)[\cos\theta \sin^3\theta(I_{0012} - I_{1112}) - \cos^3\theta \sin\theta E_{11}(I_{0022} - I_{1122})$$

$$+ \cos\theta \sin\theta(\cos^2\theta - \sin^2\theta)E_{11}(I_{0122} - I_{1222}) + 2\cos\theta \sin\theta(\cos^2\theta$$

$$- \sin^2\theta)(I_{0021} - 2I_{1121} + I_{2221})](1/L_y^2)[\sin\theta \cos^3\theta(I_{0012} - I_{1112})$$

$$- \sin^3\theta\cos\theta E_{11}(I_{0022} - I_{1122}) - \cos\theta\sin\theta(\cos^2 j - \sin^2 j)E_{11}(I_{0122} - I_{1222}) - 2\cos\theta\sin\theta(\cos^2\theta - \sin^2\theta)(I_{0021} - 2I_{1121} + I_{2221})]$$

$$B_{18} = (1/L_x^2)[\cos\theta\sin^3\theta(I_{0012} - I_{1112}) - \cos^3\theta\sin\theta E_{11}(I_{0022} - I_{1122}) + \cos\theta\sin\theta(\cos^2\theta - \sin^2\theta)E_{11}(I_{0122} - I_{1222}) + 2\cos\theta\sin\theta(\cos^2\theta - \sin^2\theta)(I_{0021} - 2I_{1121} + I_{2221})](4/L_y^2)[\sin\theta\cos^3\theta(I_{0012} - I_{1112}) - \sin^3\theta\cos\theta E_{11}(I_{0022} - I_{1122}) - \cos\theta\sin\theta(\cos^2 j - \sin^2 j)E_{11}(I_{0122} - I_{1222}) - 2\cos\theta\sin\theta(\cos^2\theta - \sin^2\theta)(I_{0021} - 2I_{1121} + I_{2221})] \quad \text{(A-3-3)}$$

APPENDIX 4

The expanded form of Equation (2-3-2a) for the cross-ply laminate is:

$$4\pi^4[P_1^2 I_{0002} + P_2^2 I_{0022} + P_3^2 I_{0222} + P_4^2(I_{0020} - 2I_{1120} + I_{2220}) + 2P_1P_2 I_{0012} + 2P_1P_3 I_{0112} + 2P_1P_4(I_{0011} - I_{1111}) + 2P_2P_3 I_{0122} + 2P_2P_4(I_{0021} - I_{1121}) + 2P_3P_4(I_{0121} - I_{1221})] - 5\pi^2[(N_x/L_x^2) - (N_y/L_y^2)][P_1(I_{0012} - I_{1112}) + P_2(I_{0022} - I_{1122}) + P_3(I_{0122} - I_{1222}) + P_4(I_{0021} - 2I_{1121} + I_{2221})] + [(N_x/L_x^2) - (N_y/L_y^2)]^2(I_{0022} - 2I_{1122} + I_{2222}) - [64N_{xy}/(9\pi^2 L_x L_y)]^2(I_{0022} - 2I_{1122} + I_{2222}) = 0 \quad \text{(A-4-1)}$$

where

$$P_1 = 2t^3/(3L_x^4) + 14t^3/(3L_y^4)$$

$$P_2 = 14t^3/(3L_x^4) + 2t^3/(3L_y^4)$$

$$P_3 = 32E_{11}t^3/(3L_x^2L_y^2)$$

$$P_4 = 64t^3/(3L_x^2L_y^2) \quad \text{(A-4-2)}$$

The expanded form of Equation (2-3-2b) for the cross ply laminate is:

$$\pi^4[Q_1Q_5 I_{0002} + Q_4Q_8 I_{0022} + Q_2Q_6 I_{0222} + Q_3Q_7(I_{0020} - 2I_{1120} + I_{2220}) + (Q_1Q_8 + Q_4Q_5)I_{0012} + (Q_1Q_6 + Q_5Q_2)I_{0112} + (Q_1Q_7$$

$$+ Q_5Q_3)(I_{0011} - I_{1111}) + (Q_4Q_6 + Q_8Q_2)I_{0122} + (Q_4Q_7$$

$$+ Q_8Q_3)(I_{0021} - I_{1121}) + (Q_2Q_7 + Q_6Q_3)(I_{0122} - I_{1222})]$$

$$- \pi^2(N_x/L_x^2)[(4Q_1 + Q_5)(I_{0012} - I_{1112}) + (4Q_4 + Q_8)(I_{0022}$$

$$- I_{1122}) + (4Q_2 + Q_6)(I_{0122} - I_{1222}) + (4Q_3 + Q_7)(I_{0021}$$

$$- 2I_{1121} + I_{2221})] - \pi^2(N_y/L_y^2)[(Q_1 + 4Q_5)(I_{0012} - I_{1112})$$

$$+ (Q_4 + 4Q_8)(I_{0022} - I_{1122}) + (Q_2 + 4Q_6)(I_{0122} - I_{1222}) + (Q_3$$

$$+ 4Q_7)(I_{0021} - 2I_{1121} + I_{2221})] + [(4N_x^2/L_x^4 + 17N_xN_y/(L_x^2L_y^2)$$

$$+ 4N_y^2/L_y^4](I_{0022} - 2I_{1122} + I_{222}) + [128N_{xy}(9\pi^2L_xL_y)]^2(I_{0022}$$

$$- 2I_{1122} + I_{2222}) = 0 \qquad \text{(A-4-3)}$$

where

$$Q_1 = (2t^3/3)(1/L_x^4 + 112/L_y^4)$$

$$Q_2 = 128t^3E_{11}/(3L_x^2L_y^2)$$

$$Q_3 = 256t^3/(3L_x^2L_y^2)$$

$$Q_4 = (2t^3/3)E_{11}(7/L_x^4 + 16/L_y^4)$$

$$Q_5 = (2t^3/3)(16/L_x^4 + 7/L_y^4)$$

$$Q_6 = 128t^3E_{11}/(3L_x^2L_y^2)$$

$$Q_7 = 256t^3/(3L_x^2L_y^2)$$

$$Q_8 = (2t^3/3)E_{11}(7/L_x^4 + 16/L_y^4) \qquad \text{(A-4-4)}$$

APPENDIX 5

$$\begin{bmatrix} \dfrac{\pi^2L_xL_y}{4}\left(\pi^2F_{11} - \dfrac{N_x}{L_x^2} - \dfrac{N_y}{L_y^2}\right) - \dfrac{32}{9}(8\pi^2S_{11} + N_{xy}) & \\ - \dfrac{32}{9}(2\pi^2S_{11} + N_{xy}) & \pi^2L_xL_y\left(4\pi^2F_{11} - \dfrac{N_x}{L_x^2} - \dfrac{N_y}{L_y^2}\right) \end{bmatrix} \begin{bmatrix} c_{11} \\ c_{22} \end{bmatrix} = 0 \qquad \text{(A-5-1)}$$

$$\begin{bmatrix} \dfrac{\pi^2 L_x L_y}{4}\left(\pi^2 F_{12} - \dfrac{N_x}{L_x^2} - \dfrac{4N_y}{L_y^2}\right) - \dfrac{32}{9}(2\pi^2 S_{21} + N_{xy}) \\ -\dfrac{32}{9}(2\pi^2 S_{12} + N_{xy}) \quad \dfrac{\pi^2 L_x L_y}{4}\left(\pi^2 F_{21} - \dfrac{4N_x}{L_x^2} - \dfrac{N_y}{L_y^2}\right) \end{bmatrix} \begin{bmatrix} c_{12} \\ c_{21} \end{bmatrix} = 0 \quad \text{(A-5-2)}$$

Using either one of two equations in above each equation, the mode shape ratio can be obtained.

Equation to solve for the time-dependent mode ratio c_{12}/c_{21} for the angle-ply laminates is:

$$\begin{aligned}
&[9\pi^2 L_x L_y/128][(\pi^2/L_x^4)\{\sin^4\theta I_{0012} + 2\cos^2\theta\sin^2\theta E_{11} I_{0122} + 4\cos^2\theta\sin^2\theta \\
&\times (I_{0021} - I_{1121}) + E_{11}\cos^4\theta I_{0022}\} + \{8\pi^2/(L_x^2 L_y^2)\}\{E_{11}(\sin^4\theta \\
&+ \cos^4\theta) I_{0122} + \sin^2\theta\cos\theta(E_{11} I_{0022} + I_{0012} - 4I_{0021} + 4I21_{121})\} \\
&+ \{16\pi^2/(L_x^2 L_y^2)\}\{\sin^2\theta\cos^2\theta(E_{11} I_{0022} + I_{0012} - 2E_{11} I_{0122}) \\
&+ (\cos^2\theta - \sin^2\theta)^2(I_{0021} - I_{1121})\}\{16\pi^2/(L_y^4)\}\{\sin^4\theta E_{11} I_{0022} \\
&+ 2\cos^2\theta\sin^2\theta E_{11} I_{0122} + 4\cos^2\theta\sin^2\theta(I_{0021} - I_{1121}) \\
&+ \cos^4\theta I_{0012}\} - \{3/(2t^3)\}(N_x/L_x^2 + 4N_y/L_y^2)(I_{0022} - I_{1122})]c_{12} \\
&+ (2/3)\pi^2[(1/L_x^2)\{\cos\theta\sin^3\theta I_{0012} - \cos^3\theta\sin\theta E_{11} I_{0022} \\
&+ \cos\theta\sin\theta(\cos^2\theta - \sin^2\theta)(E_{11} I_{0122} + 2I_{0021} \\
&- 2I_{1121})\}(1/L_y^2)\{\cos\theta\sin^3\theta I_{0012} - \cos^3\theta\sin\theta E_{11} I_{0022} \\
&- \cos\theta\sin\theta(\cos^2\theta - \sin^2\theta)(E_{11} I_{0122} + 2I_{0021} - 2I_{1121})\}]c_{21} \\
&- [3/(2t^3)]N_{xy}(I_{0022} - I_{1122})c_{21} = 0 \qquad \text{(A-5-1)}
\end{aligned}$$

Equation for the time-dependent mode ratio c_{11}/c_{22} of the cross-ply laminates is:

$$\begin{aligned}
&\pi^2 L_x L_y/4[p^2\{P_1(I_{0012} - I_{1112}) + P_2(I_{0022} - I_{1122}) + P_3(I_{0122} - I_{1222}) \\
&+ P_4(I_{0021} - 2I_{1121} + I_{2221})\} - (N_x/L_x^2 + N_y/L_y^2)(I_{0022} \\
&- 2I_{1122} + I_{2222})]c_{11} - (32/9)N_{xy}(I_{0022} - 2I_{1122} \\
&+ I_{2222})c_{22} = 0 \qquad \text{(A-5-2)}
\end{aligned}$$

Equation for the mode ratio c_{12}/c_{21} of the cross-ply laminates is:

$$\pi^2 L_x L_y/4[p^2\{(4Q_1 + Q_5)(I_{0012} - I_{1112}) + (4Q_4 + Q_8)(I_{0022} - I_{1122}) + (4Q_2 + Q_8)(I_{0122} - I_{1222}) + (4Q_3 + Q_7)(I_{0021} - 2I_{1121} + I_{2221})\} - (N_x/L_x^2 + 4N_y/L_y^2)(I_{0022} - 2I_{1122} + I_{2222})]c_{12} - (32/9)N_{xy}(I_{0022} - 2I_{1122} + I_{2222})c_{21} = 0 \quad \text{(A-5-3)}$$

where the constants P_i and Q_i are the same as those in Appendix 4.

5. REFERENCES

1. Hashin, Z. "Analysis of Properties of Fiber Composites with Anisotropic Constituents," *Journal of Applied Mechanics*, 46:543 (1979).
2. Massonet, Ch. "Buckling Behavior of Imperfect Elastic and Linearly Viscoelastic Structures," *International Journal of Solids and Structures*, 10:755 (1974).
3. Lekhnitskii, S. G. *Anisotropic Plates*. New York, NY:Gorden and Breach Science Publishers, pp. 382, 437 (1968).
4. Williams, J. G. *Stress Analysis of Polymers*. London, UK:Longman Group Limited, p. 148 (1973).
5. Powell, P. C. "Principle for Using Design Data," in *Thermoplastics*. R. M. Ogorkiewicz, ed. Cleveland, OH:CRC Press, p. 211 (1969).
6. Flugge, W. *Viscoelasticity*. Waltham, MA:Blaisdell Pub. Co., p. 92 (1967).
7. Hilton, H. H. "Creep Collapse of Viscoelastic Columns with Initial Curvatures," *Journal of Aeronautical Sciences*, 19:844 (1952).
8. Freudenthal, A. M. *The Inelastic Behavior of Engineering Materials and Structures*. New York, NY:John Wiley & Sons, Inc., p. 506 (1950).
9. Fiacco, A. V. and G. P. McCormick. *Nonlinear Programming—Sequential Unconstrained Minimization Techniques*. New York, NY:John Wiley & Sons (1968).
10. Hoff, N. J. "Buckling and Stability," *Journal of the Royal Aeronautical Society*, 58(517):1 (1954).
11. Yamamoto, Y. "Considerations of a Stability Criterion for Creep Buckling," *Journal of Mechanics and Physics of Solids*, 18:165 (1970).
12. Ross, A. D. "The Effects of Creep of Instability and Indeterminacy Investigated by Plastic Models," *The Journal of the Institution of Structural Engineers*, 24:421 (August 1946).
13. Vinogradov, A. M. "Buckling of Viscoelastic Beam-Columns," *27th Structural Dynamics and Materials Conference*, American Institute of Aeronautics and Astronautics Inc., 1:502 (1986).
14. Booker, J. R. et al. "Stability of Viscoelastic Structural Members," *Civil Engineering Transactions*, p. 45 (1974).
15. Booker, J. R. "A Method of Solution for the Creep Buckling of Structural Members of a Linear Viscoelastic Material," *Journal of Engineering Mathematics*, 7(2):101 (April 1973).
16. Lin, T. H. "Stress in Columns with Time Dependent Elasticity," *Proceedings of the 1st Midwestern Conference on Solid Mechanics*, p. 196 (1953).
17. Miyase, A., A. W.-L. Chen, P. H. Geil and S. S. Wang. "Anelastic Deformation and Fracture of Thermoplastic-Matrix Fiber Composite at Elevated Temperature, Part II Undirectional Composite Laminate," American Chemical Society 20th Great Lake Regional Meeting, Milwaukee (June 1986).
18. Froberg, C.-E. *Introduction to Numerical Analysis, 2nd ed.* Reading, MA:Addison-Wesley Publishing Company, p. 348 (1969).

19. Ferry, J. D. *Viscoelastic Properties of Polymers*. New York, NY, section 11 (1970).
20. Wang, S. S., E. C. Klang, A. Miyase and A. Dasgupta. "Viscoelastic Shear Behavior of the Thermoplastic Matrix Composite at Elevated Temperatures," ASME, Winter Annual Meeting, Boston (December 1987).
21. Wilson, D. W. and J. R. Vinson. "Viscoelastic Buckling Analysis of Laminated Composite Columns," *Recent Advances in Composites in the United States and Japan*, ASTM STP 864, J. R. Vinson and M. Taya, editors, American Society for Testing and Materials, Philadelphia, p. 368 (1985).
22. Wang, S. S., A. Miyase, P. H. Geil and A. Chen. "Anelastic Deformation and Fracture of Thermoplastic Matrix Composites at Elevated Temperatures" (1988).